

Article

Machine Learning Applied to K-Bentonite Geochemistry for Identification and Correlation: The Ordovician Hagan K-Bentonite Complex Case Study

Achim D. Herrmann ^{1,*}, John T. Haynes ² , Richard M. Robinet ¹ and Norlene R. Emerson ³

¹ Department of Geology & Geophysics and Coastal Studies Institute, Louisiana State University, Baton Rouge, LA 70803, USA; rrobi65@lsu.edu

² Department of Geology and Environmental Science, James Madison University, MSC 6903, Harrisonburg, VA 22807, USA; haynesjx@jmu.edu

³ Department of Geography & Geology, University of Wisconsin—Richland, Richland Center, WI 5358, USA; emersonn@uwplatt.edu

* Correspondence: aherrmann@lsu.edu; Tel.: +1-225-578-3016

Abstract: Altered tephtras (K-bentonites) are of great importance for calibration of the geologic time scale, for local, regional, and global correlations, and paleoenvironmental reconstructions. Thus, definitive identification of individual tephtras is critical. Single crystal geochemistry has been used to differentiate tephtra layers, and apatite is one of the phenocrysts commonly occurring in tephtras that has been widely used. Here, we use existing and newly acquired analytical datasets (electron probe micro-analyzer [EPMA] data and laser ablation ICP-MS [LA-ICP-MS] data, respectively) of apatite in several Ordovician K-bentonites that were collected from localities about 1200 km apart (Minnesota/Iowa/Wisconsin and Alabama, United States) to test the use of machine-learning (ML) techniques to identify with confidence individual tephtra layers. Our results show that the decision tree based on EPMA data uses the elemental concentration patterns of Mg, Mn, and Cl, consistent with previous studies that emphasizes the utility of these elements for distinguishing Ordovician K-bentonites. Differences in the experimental setups of the analyses, however, can lead to offsets in absolute elemental concentrations that can have a significant impact on the correct identification and correlation of individual K-bentonite beds. The ML model using LA-ICP-MS data was able to identify several K-bentonites in the southern Appalachians and establish links to K-bentonites samples from the Upper Mississippi Valley. Furthermore, the ML model identified individual layers of multiphase eruptions, thus illustrating very well the great potential of applying ML techniques to tephrochronology.

Keywords: tephrochronology; tephrostratigraphy; tephtra fingerprinting; Deicke; Millbrig; Dick-eyville; Elkport



Citation: Herrmann, A.D.; Haynes, J.T.; Robinet, R.M.; Emerson, N.R. Machine Learning Applied to K-Bentonite Geochemistry for Identification and Correlation: The Ordovician Hagan K-Bentonite Complex Case Study. *Geosciences* **2021**, *11*, 380. <https://doi.org/10.3390/geosciences11090380>

Academic Editors: Roberto Moretti and Jesus Martinez-Frias

Received: 23 July 2021

Accepted: 31 August 2021

Published: 9 September 2021

Publisher's Note: MDPI stays neutral with regard to jurisdictional claims in published maps and institutional affiliations.



Copyright: © 2021 by the authors. Licensee MDPI, Basel, Switzerland. This article is an open access article distributed under the terms and conditions of the Creative Commons Attribution (CC BY) license (<https://creativecommons.org/licenses/by/4.0/>).

1. Introduction

The geochemistry of igneous apatite is complex, and in response to various magmatic conditions during crystallization (e.g., oxygen fugacity, temperature, crystallization rate, chemical composition), its trace-element composition can acquire a characteristic geochemical fingerprint [1,2]. Because of this, the geochemistry of apatite is a powerful tool for testing tectonostratigraphic hypotheses and for the high-resolution correlation of pyroclastics produced by large volcanic eruptions, as demonstrated by its successful use in many investigations of tephtras ranging in age from the Paleozoic to the recent Cenozoic [3–6].

Explosive volcanism during the later Ordovician (470–445 Ma; Figures 1 and 2) resulted in many airfall deposits of volcanic ash being spread across much of what is now eastern North America [7–9], northern Eurasia [10,11], and western South America [12]. It has long been recognized that the geochemistry of these Ordovician K-bentonites can

be used for high-resolution stratigraphy [4,13]. The tephrochronological approach has led to development of a high-resolution framework useful for identifying and correlating stratigraphic packages that are otherwise difficult to identify. For instance, much stratigraphic correlation in the northern part of Laurentia (Figure 1) is based on K-bentonite tephrostratigraphy [4,5,14,15]. Most importantly, a high-resolution stratigraphic framework based on apatite phenocryst geochemistry facilitates testing of stratigraphic and geological hypotheses, e.g., apatite geochemistry provided evidence that the stratigraphic changes across the Sandbian-Katian boundary are time-transgressive across part of the Appalachian basin and therefore are most likely not global events [5].

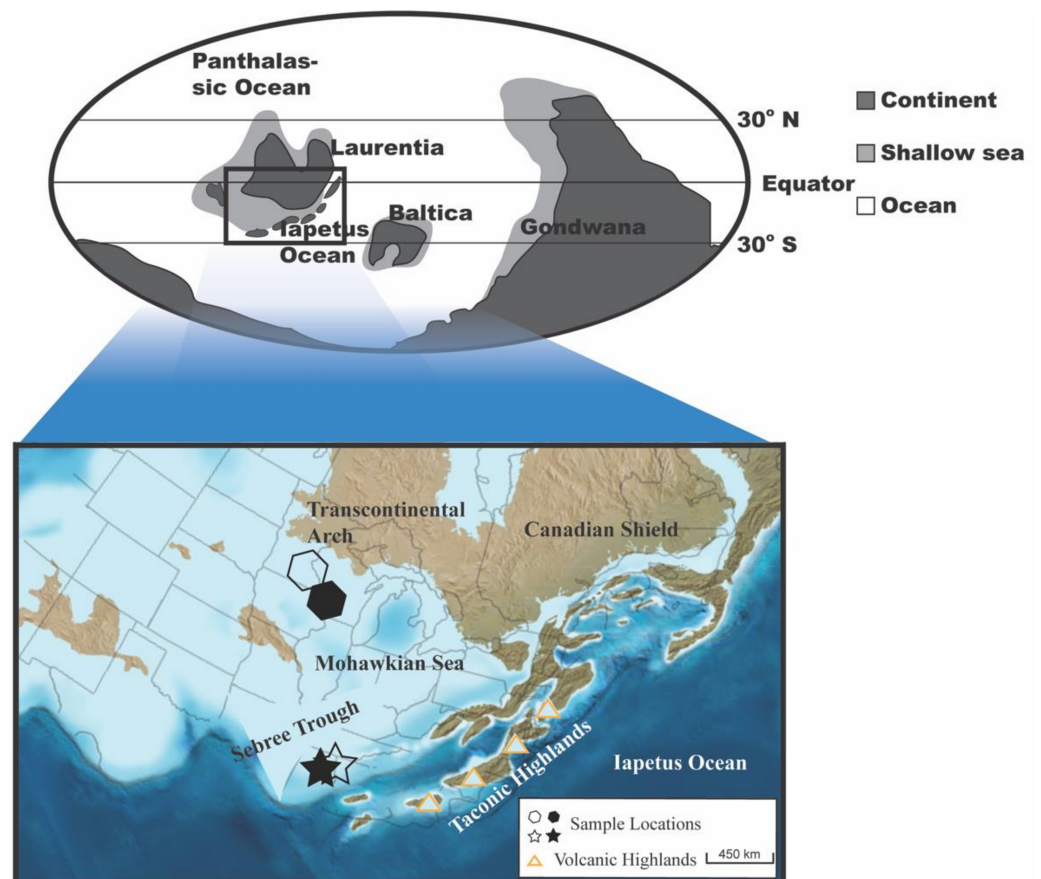


Figure 1. Paleogeographic setting: Full star—location of Big Ridge and Bruton Gap sections, open star—location of Tidwell Hollow and Fort Payne sections, all in Alabama, full octagon—location of Decorah and Dickeyville sections, open octagon—location of Rochester and St. Paul sections, both in Minnesota. Regional Ordovician paleogeography modified from [22].

Those tephras, several of which were generated by arguably the largest explosive volcanic eruptions in the Phanerozoic, have been altered to K-bentonites, including three of the K-bentonite beds in the Hagan K-bentonite complex [16] of eastern North America (Deicke, Millbrig, and Elkport) that are the subject of our investigations reported herein. In recent years, machine-learning techniques (hereinafter ML) have been applied to volcanology [17,18]. Here, we test whether ML techniques can be applied to these deposits to enhance our ability to identify and correlate these eruptive events that could be used to track environmental and tectonic changes through time and space in order to test tectonostratigraphic hypotheses [5,19–21].

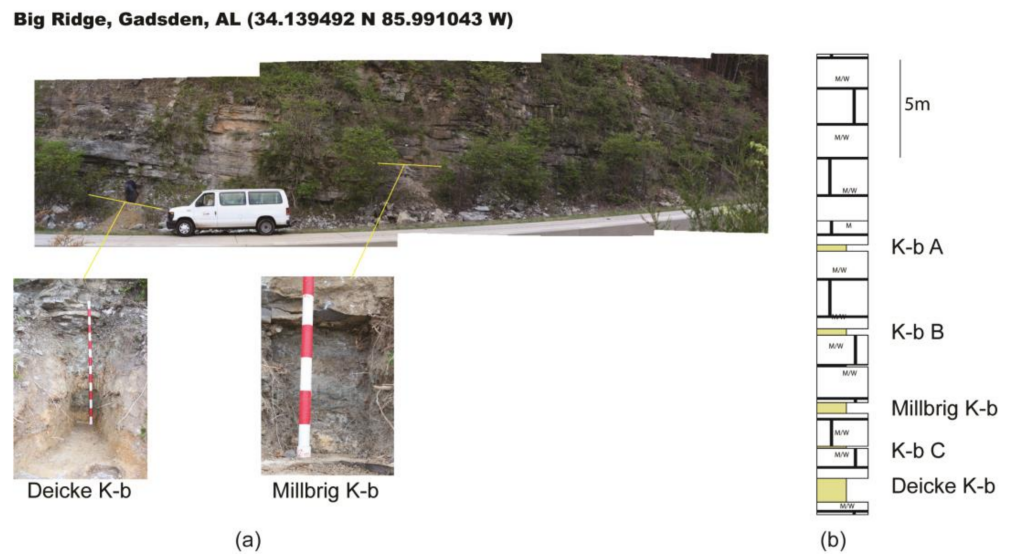


Figure 2. (a) The exposure of outcropping K-bentonites at Big Ridge, with insets of the Deicke and Millbrig K-bentonites showing the individual distinct layers that are evident subsequent to being completely excavated prior to collecting samples from each visibly different layer. (b) Stratigraphic column of the Big Ridge section, showing the stratigraphic horizons of individual K-bentonites used for developing the identification model using LA-ICP-MS data. K-b = K-bentonite. Recessed intervals (yellow) are K-bentonites. M: Mudstone; M/W: Mud/Wackestone. Red and white intervals on Jacob’s Staff are 10 cm each.

2. Materials and Methods

2.1. Machine Learning Environment and Parameters

We used the open-access machine-learning software WEKA [23,24] for these analyses. WEKA is widely used and has appropriate analytical tools for machine-learning applications for decision tree generation based on geochemical datasets [25]. Datasets were imported and, depending on the geochemical dataset, processed as follows. Datasets were processed similarly, as outlined below.

We built a model based on the Emerson et al. [15] dataset, which we call the “UMV (Upper Mississippi Valley)-Model”. For developing this “UMV-Model”, we used the J48 algorithm for generating our decision trees. The J48 algorithm is the java software implementation of the C4.5 classifier [26] in WEKA, and it is an algorithm that aims at choosing the particular attribute of the data which most effectively splits its set of samples into subsets at each node of the decision tree. The resulting decision tree was pruned by forcing 15 instances into a leaf, thereby not overfitting the results. The dataset of Emerson et al. [15] is already published, and can be accessed through their manuscript location.

We also developed the “Big-Ridge-Model”, which is based on laser ablation-inductively coupled plasma-mass spectrometry (hereinafter LA-ICP-MS) data of newly and previously reported apatite phenocrysts. We also used the J48 tree-building algorithm, and, as with the EPMA data, the resulting decision tree was pruned by forcing 15 instances into a leaf, thereby not overfitting the results (Figure 3). The dataset is available in Appendix A.

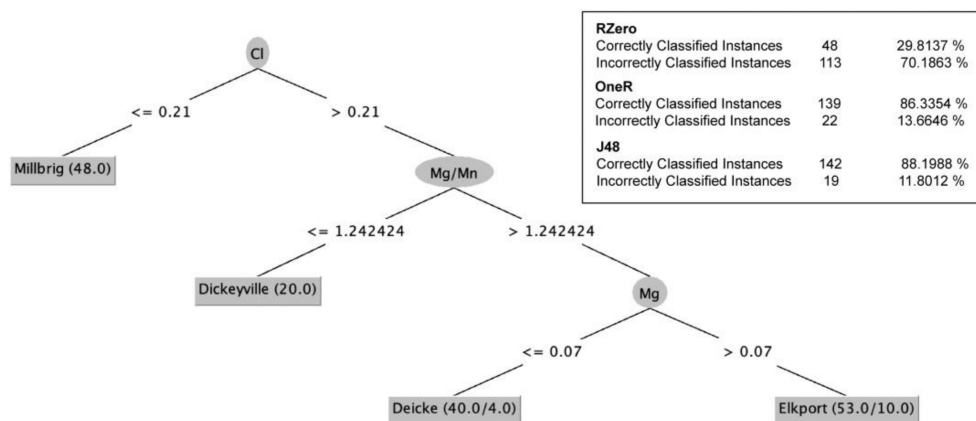


Figure 3. UMV-model decision tree of four prominent Ordovician K-bentonites using the J48 classifier. Shown in the inset are the percentages for correctly and incorrectly classified instances on different decision modes. RZero: essentially guessing the most abundant class for every instance; OneR: classifying each instance based on only one variable.

2.2. Training and Test Set for Geochemical Data Based on LA-ICP-MS Data of Ordovician K-Bentonites

Table 1 presents the location information for the Ordovician K-bentonite samples in this study that were investigated using LA-ICP-MS of apatite phenocrysts and then used for the training and testing datasets for the laser ablation data. At Big Ridge (Figure 2), the Deicke K-bentonite was divided into seven visually distinct intervals (D1–D7 from base to top) and the Millbrig K-bentonite was divided into four evenly spaced and visually distinct intervals (M1–M4 from base to top).

Table 1. Location information for each sample, the name of each K-bentonite that was collected at each section, and the key references for each sample. “?” refers to K-bentonites that have been tentatively identified, but not yet geochemically fingerprinted.

Location	K-Bentonite	Key Reference	GPS Location
Big Ridge, Alabama	Deicke, Millbrig	[27]	lat. 34.13990 N long. 85.99102 W
Decorah, Iowa	Deicke	[15]	lat. 43.290249 N long. 91.765676 W
Dickeyville, Wisconsin	Millbrig, Elkport	[15]	lat. 42.661833 N long. 90.656099 W
Rochester, Minnesota	Deicke, Millbrig	[15]	lat. 43.972161 N long. 92.382820 W
St. Paul, Minnesota	Deicke, Millbrig	[28]	lat. 44.920746 N long. 93.110729 W
Fort Payne, Alabama	?	[29]	lat. 34.480380 N long. 85.709067 W
Tidwell Hollow, Alabama	?	[29]	lat. 33.87806 N long. 86.57555 W
Bruton Gap, Alabama	?	[30]	lat. 34.091294 N long. 86.041315 W

2.3. Training Set for Geochemical Data Based on Electron Probe Micro-Analyzer (EPMA)

We used the dataset of Emerson et al. [15] for the training set for testing the correlation of K-bentonites using existing EPMA data, and we used a subset of that dataset for the LA-ICP-MS test. That study focused on the geochemistry of apatite phenocrysts of four prominent Katian-Sandbian age K-bentonites recognized within the Decorah Formation in the upper Mississippi Valley states of Minnesota, Iowa, and Wisconsin (Figure 1). These K-bentonites are the Deicke, Millbrig, Elkport, and Dickeyville K-bentonites. Emerson et al. [15] reported results based on apatite phenocrysts that had been analyzed for 15 elements, and we are using only the datapoints that included Mg and Mn values, as these

two elements had been identified before as being especially informative and important when using apatite geochemistry for stratigraphic purposes.

2.4. Cross Calibration Datasets for Geochemical Data Based on Electron Probe Micro-Analyser (EPMA)

We evaluated the training model that was derived from the Emerson et al. [15] dataset with the dataset of Carey et al. [14]. Both studies analyzed distinct K-bentonite layers, some of which had previously been independently identified as the Deicke K-bentonite, or the Millbrig K-bentonite, through detailed correlation using wire-line logs, stratigraphic position, and (or) mineral content and geochemistry [7,30]. Thus, the Deicke and Millbrig samples from those studies are suitable for use as a test set, because their identification is confidently known. We used all analyzed elements and replaced missing values that were included in the Emerson et al. [15] dataset, but not in Carey et al. [14], as missing data values.

For data from the Carey et al. [14] study, we first focused on the Deicke and Millbrig K-bentonites to assess the accuracy of the UMV-model for identifying those two major K-bentonites. The dataset of Carey et al. [14] is also already published, and can be accessed through their manuscript location.

2.5. LA-ICP-MS Analysis of Apatite Phenocrysts to Establish the Training and Testing Datasets

We used the LA-ICP-MS data set from Big Ridge (Figure 1) for the training set (Big-Ridge-Model). These K-bentonites include the two thickest and most prominent ones that have previously been identified as the Deicke and Millbrig K-bentonite beds [30], as well as three previously unnamed K-bentonites (Kb-A, Kb-B, and Kb-C). The LA-ICP-MS analyses were performed using a Thermo iCap Qc ICP-MS that was connected to a Cetac G2-213 Nd:YAG laser system in the Department of Geology and Geophysics at Louisiana State University. Isotopes of individual elements analyzed included ^{24}Mg , ^{43}Ca , ^{55}Mn , ^{57}Fe , ^{89}Y , ^{232}Th , ^{238}U and the rare earth elements La-Lu. Elemental concentrations were normalized against the NIST612 glass standard, using ^{43}Ca as an internal standard using Iolite 2.5 [31]. During preprocessing, we eliminated data points with inclusions or other problems during the laser ablation session. Durango and Madagascar (MAD) apatites were used as secondary standards. Additional sample processing and analytical details were reported by Herrmann et al. [27]. The results of the LA-ICP-MS analyses used for the training set are tabulated in online Appendix A. The results of the LA-ICP-MS analyses for the testing set are tabulated in online Appendix B. The laser parameters for the individual runs are in Appendix C. The model was derived using the following 15 attributes based on elemental concentrations and different ratios: Mg, Mn, Y, U, REEsum, $(\text{La}/\text{Sm})_{\text{N}}$, $(\text{La}/\text{Yb})_{\text{N}}$, Pr/Pr^* , Ce/Ce^* , La/La^* , Eu/Eu^* , Mn/Eu^* , Mg/Mn , Ce^*/Y , and $(\text{Gd}+\text{Sm})/\text{Mn}$. Rare earth elements were normalized to average chondrite values [32].

3. Results

3.1. Machine-Learned Model for Distinguishing Four Prominent Ordovician K-Bentonites Based on EPMA data

3.1.1. Model Results for the UMV-Model

We built the UMV-model based on the Emerson et al. [15] dataset (Figure 3).

3.1.2. Cross-Validation of the UMV-Model Using the Carey Dataset

The UMV-model has distinct differences in identifying the Deicke and Millbrig K-bentonite correctly (Table 2; Figure 3). We treated the data from the known Deicke and Millbrig K-bentonite locations of Carey et al. [14] as unknowns to test the UMV-model. The Deicke K-bentonite was much more reliably identified than the Millbrig K-bentonite. In particular, cut-off values of Cl concentrations and Mg/Mn ratios led to misidentification on the fringes of individual data clusters (Figure 4).

Table 2. Cross-validation results of UMV-model using the Carey et al. [14] dataset. Columns indicate the percentage of identification based on model.

K-Bentonite Identified by Carey et al. [14]	Deicke	Millbrig	Elkport	Dickeyville
Deicke (n = 405)	94.6%	2.2%	1.0%	2.2%
Millbrig (n = 438)	3.2%	84.0%	3.9%	8.9%

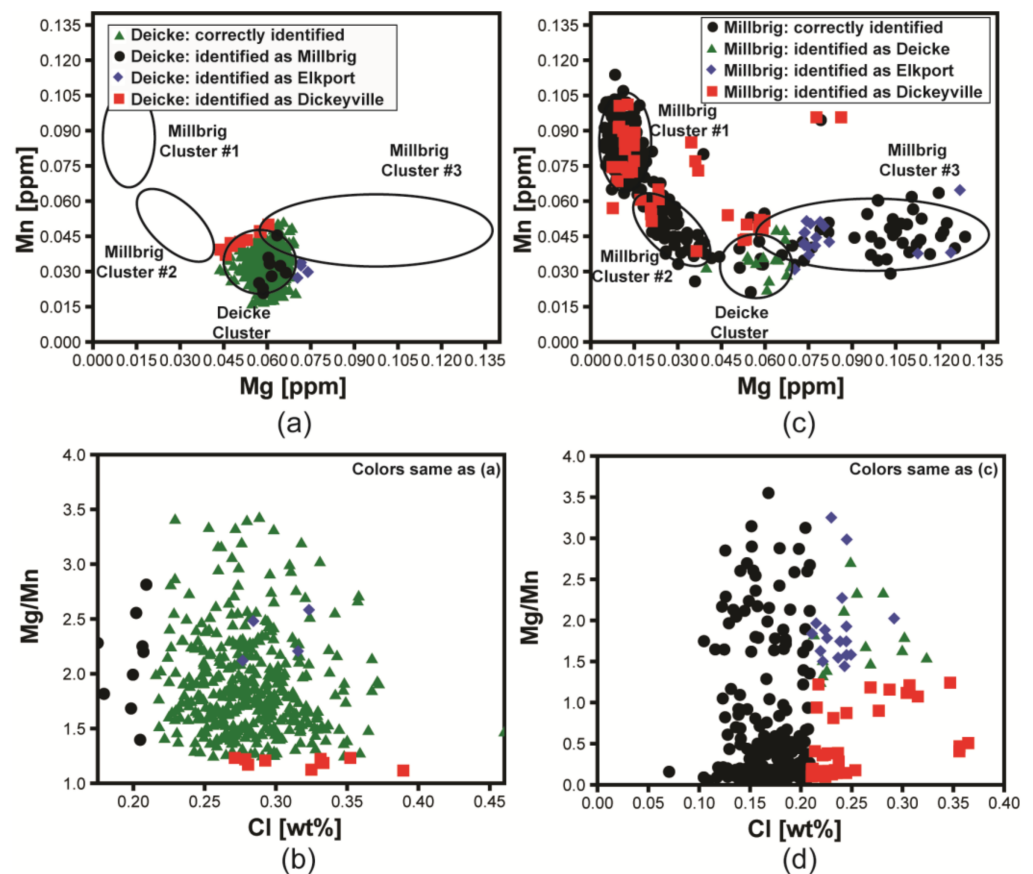


Figure 4. Identification of misidentified Deicke and Millbrig samples from the dataset of Carey et al. [14] using the dataset of Emerson et al. [15] as the training dataset. (a) Clustering of Deicke samples in Mg–Mn space; (b) Clustering of Deicke samples in Cl–Mg/Mn space. (c) Clustering of Millbrig samples in Mg–Mn space; (d) Clustering of Millbrig samples in Cl–Mg/Mn space. The misidentifications are due to offsets in Cl, Mn, and Mg concentrations were chosen by the ML algorithm as cut-offs. In particular the Cl concentration cut-off at 0.21 leads to the most misidentified Millbrig as well as misidentified Deicke samples. The Millbrig and Deicke clusters shown in (a,c) are from Carey et al. [14]. Mn and Mg concentrations are in PPM and Cl concentration is in weight %.

3.2. Machine-Learned Model for Distinguishing Ordovician K-Bentonites Based on LA-ICP-MS Data from Big Ridge, AL

3.2.1. Cross-Validation of the LA-ICP-MS-Model using the Known K-Bentonites from the Upper Mississippi Valley

There is no available LA-ICP-MS dataset that can be used for cross-validation similar to the cross-validation of the UMV-model. Although Sell et al. [5] analyzed apatite phenocrysts from K-bentonites using LA-ICP-MS, the available dataset that is part of the supplementary online material accompanying that 2015 paper unfortunately lacks data for critical elements (e.g., Mg) that were reported by the authors to have been obtained from analyses of several specific K-bentonite samples that are of interest herein, thus preventing us from making a meaningful comparison. Therefore, we analyzed a subset of the apatite

phenocrysts from well-known K-bentonites in the UMV (Figure 1) that are equivalent to the samples published by Emerson et al. [15]. The results are shown in Figures 5 and 6, and these new data are available in online Appendix B.

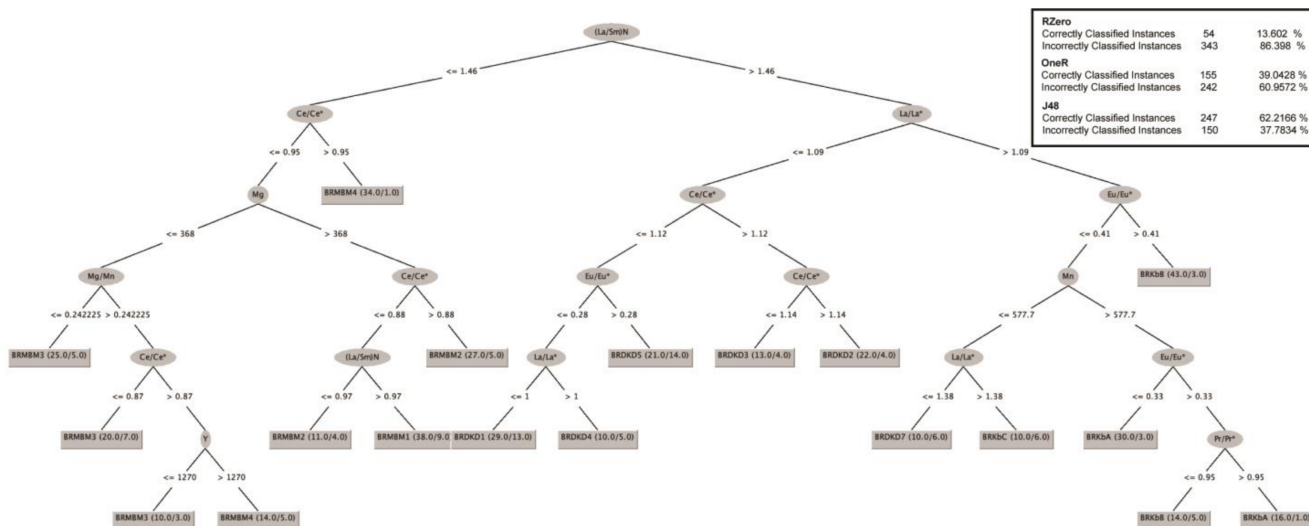


Figure 5. Big-Ridge-Model decision tree of five Ordovician K-bentonites exposed in outcrop at Big Ridge using the J48 classifier. Shown in the inset are the percentages for correctly and incorrectly classified instances based on different decision modes. RZero: essentially guessing the most abundant class for every instance; OneR: classifying each instance based on only one variable.

The Deicke K-bentonite samples from Minnesota (St. Paul and Rochester locations), and Iowa (Decorah location) are identified by the model. Only the sample from Decorah includes predictions that are not originating from one of the Deicke horizons at Big Ridge. The majority of instances in the samples from St. Paul and Rochester appear to come from horizon D5. At Decorah, the majority of instances are consistent with horizon D7 at Big Ridge. The minority of samples have an affinity with the lower horizons of the Deicke at Big Ridge (D1–D4).

The Millbrig K-bentonite samples from the St. Paul and Rochester sections are identified by the model. The majority of instances in those two samples appear to come from horizons M3 and M4. The minority of samples have an affinity with the lower horizons of the Millbrig at Big Ridge (M1–M2). Only one misidentified sample occurs in the Rochester sample.

The Elkport K-bentonite sample from the Dickeyville, WI section has a majority of Kb-B affinity, however it also has several instances from all other K-bentonites at Big Ridge.

3.2.2. Identification of Unknown K-Bentonites in the Southern Appalachians Using the Big-Ridge-Model

The two K-bentonite samples from the Tidwell Hollow location have clear differences. Sample “TH ‘Millbrig’” has a majority of Millbrig horizons identified (M2–M4), while Sample “TH ‘Deicke’” has a majority of Deicke horizons identified (D1–D7). Besides Deicke horizons, there were no misidentified horizons in that sample, but the TH ‘Millbrig’ did have a minor contribution of samples that were identified as Deicke samples.

The “Fort Payne ‘Deicke’” K-bentonite samples include only predictions that are originating from different Deicke horizons at Big Ridge. The majority of instances come from horizon D5 and D1, with a minor contribution from D4.

The “Bruton Gap” K-bentonite samples include a mix of predictions that are originating from different Deicke horizons (D1 and D4) and one Millbrig horizon (M4) at Big Ridge. The majority of instances come from the Millbrig horizon.

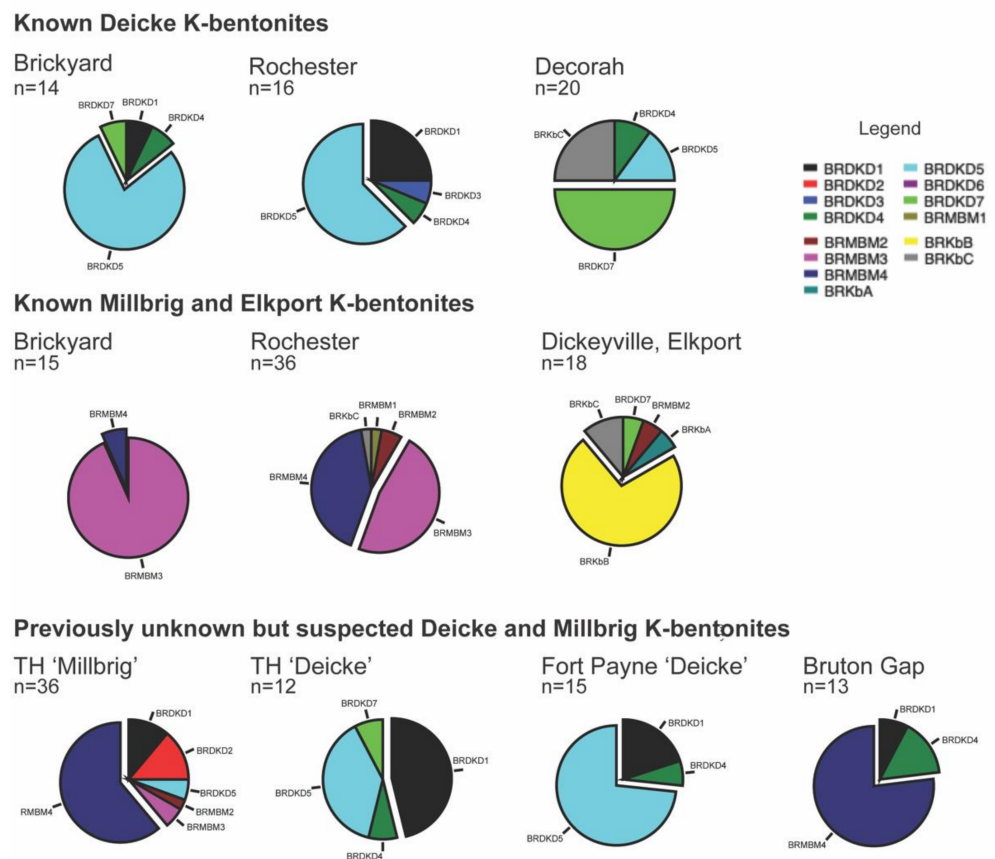


Figure 6. Identification results based on applying the Big-Ridge-Model to K-bentonite beds that had previously been identified as Deicke, Millbrig, and Elkport K-bentonites in the Upper Mississippi Valley and K-bentonite beds in the Southern Appalachians that had previously been interpreted as correlative to the K-bentonites in the Upper Mississippi Valley. ‘Brickyard’ is the informal field name of the exposure where the Deicke K-bentonite sample was collected in St. Paul, Minnesota; ‘TH’ is Tidwell Hollow, Alabama.

4. Discussion

4.1. Evaluation of the ML Models Based on Geochemical Data of Apatite Phenocrysts

The main elements that the UMV-model chooses are based on elemental concentration patterns of Mg, Mn, and Cl. This is consistent with previous suggestions that these three elements are important for distinguishing Ordovician K-bentonites [14]. Nevertheless, the different models lead to misidentifications for the following reasons.

First, different experimental setups for the analysis can lead to offsets in absolute values of the different elements. This has been shown to be an issue for Ordovician K-bentonites before [5,27]. In particular, problems of accurately quantifying Cl and F concentrations in geological samples, including apatites, using EPMA has been well documented [33,34]. Thus, offsets of data points and data point clusters caused by analytical differences can have a significant impact on the correct identification and correlation of individual K-bentonite beds.

Second, the heterogeneity of individual K-bentonites that consist of multiple tephra layers produced by different eruptions, or by different phases of the same eruption, can create problems for the correct identification of a given K-bentonite bed. The algorithm works best if discrete clusters of unique elemental concentration pairs can be found. The J48 classifier used in WEKA, which is based on the C4.5 classifier [26], is an algorithm that aims at choosing the particular attribute of the data which most effectively splits its set of samples into subsets at each node of the decision tree. At least two of the Ordovician K-bentonites, however, have been shown to be the result of multiple eruption phases that

led to distinct changes in the geochemistry of the phenocrysts of each eruptive phase. For example, on the basis of textural changes in a key exposure in Tennessee, Haynes [30] hypothesized that the Millbrig K-bentonite might consist of four individual ash falls, each with distinct lithological characteristics. This interpretation is consistent with the identification of temporal geochemical changes during the deposition of each ash layer as identified by unique clusters (Figure 3; see refs. [5,14]). More recently, Herrmann et al. [27] showed that the Deicke K-bentonite also has multiple layers, and they suggest that this finding can most likely be attributed to the amalgamation of several discrete tephra layers into one stratigraphic horizon as seen today. The type localities and type sections of the Deicke and Millbrig K-bentonites are in the Upper Mississippi Valley (UMV) and are relatively far removed from the Ordovician volcanic centers that produced these ash falls. Additionally, because the K-bentonites are much thinner in the UMV (maximum of several cm thick) than they are exposures that are closer to the volcanic centers, like the Big Ridge section (Figure 2) in Alabama (up to 1.2 m thick; [27,29]), it is conceivable that not all ash fall layers will have all known clusters represented in the more distal locations.

Third, the depositional environments along the active margin of Eastern Laurentia during the eruption of the volcano(es) responsible for producing the tephra that comprise the Hagan K-bentonite complex were highly dynamic. Locally and regionally, these include carbonate platform environments, mixed siliciclastic and carbonate environments, and strictly siliciclastic environments, all of which having been interpreted as being in relatively shallow water setting with currents that probably led to the resuspension, erosion and redeposition of the tephra that could have led to mixing of individual tephra components in what are now the K-bentonite beds of this region [21,29,30,35].

Lastly, closer to the eruption center, it would be expected that the largest phenocrysts will have been deposited. In the case of the Deicke K-bentonite, Herrmann et al. [27] also showed that significant zonation is present within apatite phenocrysts. Thus, magma evolution during the eruption can lead to geochemical zonation within individual apatite grains that at the small spot size of EPMA can lead to noise within the dataset. The generally larger spot size of LA-ICP-MS analyses tend to average these values.

4.2. Identification of Unknown K-Bentonites

4.2.1. Identification and Correlation of “K-Bentonite B” at Big Ridge

The ML model using LA-ICP-MS data was able to establish a link between a previously unnamed K-bentonite at Big Ridge (field notation K-b B; Figure 1) with the Elkport K-bentonite of the Upper Mississippi Valley. The stratigraphic location of K-b B above the Millbrig is consistent with the relative stratigraphic positions of the Millbrig and Elkport K-bentonites in the Upper Mississippi Valley. Thus, we tentatively assign K-b B as the Elkport K-bentonite, with high confidence. This allows a high-resolution correlation of K-bentonites in Alabama to be expanded from only the Deicke and Millbrig stratigraphic interval, to the younger Elkport level. This is an important finding, one that is critical to establishing an ever-more precise correlation framework for evaluating environmental changes across this interval [20,21].

4.2.2. Identification and Correlation of the Deicke and Millbrig K-Bentonites at Tidwell Hollow and Fort Payne

The ML model using LA-ICP-MS data was able to confirm the previous interpretation that the Deicke and Millbrig K-bentonites are present at Tidwell Hollow [29] and that the Deicke is present at Fort Payne [20,29,30]. Confirming the presence of these K-bentonites at Tidwell Hollow is not only important for constraining the timing of environmental changes across this interval [20,21], but also for interpreting the paleogeographic and environmental setting of this area during the later Ordovician. The observation that, despite the small dataset, essentially all Deicke and Millbrig horizons from Big Ridge can be identified at these locations, attests to the closeness to the volcanic center such that effectively no filtering of the tephra through depositional processes occurred.

4.2.3. Identification and Correlation of the Millbrig K-Bentonites at Bruton Gap

The ML model tentatively assigns the unknown K-bentonite from Bruton Gap, Alabama to the Millbrig. This unknown K-bentonite is one of five K-bentonites identified in the Bruton Gap section by Haynes [30], in particular this bed is a relatively thin K-bentonite bed that was collected upsection from the thicker K-bentonite tentatively identified as the Deicke, and downsection from the thicker biotite-rich K-bentonite tentatively identified as the Millbrig. With identification of this thinner K-bentonite as having Millbrig affinity, it is quite possible that the original stratigraphic “picks” of Haynes [30] for the Bruton Gap section should be re-evaluated and compared not with the Big Ridge section to the northeast, but with the Red Mountain Expressway section to the southwest, where lenses and discontinuous beds of limestone are intercalated with the Millbrig K-bentonite, as now seems to be the better explanation for the K-bentonite stratigraphy at Bruton Gap. Additional work is planned for further investigation of the Bruton Gap section and its precise relationships with the other sections in the region.

4.2.4. Fine-Tuning our Understanding of the Eruptive Sequence of Ordovician K-Bentonites Generated by Large Caldera Building Eruptions

At the Big Ridge section (Figure 2) the Deicke and Millbrig K-bentonites are of relatively great thickness [35], and those exposures can be confidently assumed to represent proximal, coarse-grained archives for the eruption of tephra generated during caldera building events. The Deicke and Millbrig K-bentonites at Big Ridge both reach 1–1.2 m in thickness, and both beds can be subdivided into individual layers based on lithological and mineralogical observations (Figure 2). In contrast, in the Upper Mississippi Valley, where the stratotypes for many of the prominent Ordovician K-bentonites are located [36], the altered tephra are commonly only a few cm thick at most. The majority of the Deicke and Millbrig apatite phenocrysts from UMV samples appear to have originated during the later stages of the formation of the tephra precursors that have now altered to K-bentonites. The samples from the Deicke in the UMV are dominated by horizons D5 and D7, whereas the Millbrig samples from the UMV are dominated by horizons M3 and M4. Thus, it appears that the first eruption events were smaller in scale, and the caldera forming, massive events happened at the end of each eruption. This would be consistent with previous observations of K-bentonite samples from Virginia [14] that showed changes in the eruptive sequence. Here, based on the absence of apatite phenocrysts that would be the more distal Upper Mississippi Valley time equivalents with the early stages of volcanism as documented at the more proximal Big Ridge section, we can also document that the eruptive style of the of the explosive eruptions’ later stages led to a wider dispersal of the volcanic ash. Therefore, we conclude that in samples from more distal locations relative to these volcanic centers, tephra from the early stages might be missing.

5. Conclusions

We have demonstrated how ML can be applied to a stratigraphic problem with measurable success. Using apatite phenocryst geochemical data from several Ordovician K-bentonite beds, including the well-known Deicke and Millbrig K-bentonites, which are layers of altered airfall tephra from explosive volcanic eruptions at ~454–455 Ma along the Laurentian margin, ML methodology separates and distinguishes the phenocrysts in a given K-bentonite from those in others, and our results show the value of ML in chronostratigraphy and tephrostratigraphy. Our results are also in accord with prior studies which suggested that both the Millbrig and the Deicke explosively eruptive events consisted of multiple eruptive stages. We establish with confidence that only the phenocrysts from the later stages of the eruption were deposited in the more distal regions that now comprise the many excellent exposures in the Upper Mississippi Valley, as compared with the more complete record of phenocrysts that are present in the more proximal sections of Alabama.

The Elkport K-bentonite is for the first time identified in the Big Ridge outcrop. This finding now allows for correlation of the Upper Mississippi Valley deposits into Alabama

at this chronostratigraphically precise horizon. The presence of the Deicke and Millbrig K-bentonites at Tidwell Hollow, Alabama, is confirmed. An unknown K-bentonite at Bruton Gap, Alabama, is tentatively assigned to the Millbrig, but further work is planned to confirm its position within the Bruton Gap sequence and to refine its usefulness for regional correlation.

Future work is needed to establish elemental profiles that can best be used to characterize individual K-bentonite beds based on geochemical fingerprinting. This might include elements that are not frequently analyzed in apatites so far. Finally, we note that care must be taken if samples for the training set are collected from exposures that are relatively far away from the eruption center, as such samples from a more distant location might very well not be representative of the entire eruptive sequence.

Author Contributions: Conceptualization, A.D.H. and J.T.H.; methodology, A.D.H.; J.T.H., R.M.R., N.R.E.; fieldwork and sampling, A.D.H., N.R.E., R.M.R., J.T.H.; software, A.D.H.; validation, A.D.H.; writing—original draft preparation, A.D.H., J.T.H.; data analysis and interpretation, A.D.H., J.T.H., R.M.R., N.R.E.; writing—review and editing, A.D.H., J.T.H., R.M.R., N.R.E.; funding acquisition, A.D.H. All authors have read and agreed to the published version of the manuscript.

Funding: A.D.H. acknowledges funding from the National Science Foundation (EAR-1324954). RMR thanks GEODE funding (BG-004172) from the Department of Geology and Geophysics at LSU. Part of this work is part of RMR's dissertation project at LSU, specifically LA-ICP-MS work to identify the geochemistry of apatite from K-bentonite beds.

Institutional Review Board Statement: Not applicable.

Informed Consent Statement: Not applicable.

Data Availability Statement: The data for this paper is available in the Appendices [A](#) and [B](#).

Acknowledgments: We thank the two anonymous reviewers whose comments/suggestions helped improve and clarify this manuscript.

Conflicts of Interest: The authors declare no conflict of interest. The funders had no role in the design of the study; in the collection, analyses, or interpretation of data; in the writing of the manuscript, or in the decision to publish the results.

Appendix A

LA-ICP-MS results of known Ordovician K-bentonites used for the ML training set.

Table A1. Results from the LA-ICP-MS analyses used as the training set. All elemental abundances are given in ppm.

Sample Name	Mg	Mn	Fe	Y	Th	U	La	Ce	Pr	Nd	Sm	Eu	Gd	Tb	Dy	Ho	Er	Tm	Yb	Lu
Big_Ridge_M1_1	1009	859	1079	1599	8.78	2.37	542	1326	225	1210	298	14.8	320	42.9	252	46.4	115.1	13.29	71.3	9.09
Big_Ridge_M1_2	836	757	842	1400	15.44	4.7	741	1782	297	1620	395	22.2	400	56.1	316	57.7	141.6	15.85	80.5	10.47
Big_Ridge_M1_3	1125	570	757	1409	16.5	3.75	689	1677	287	1563	386	23.2	386	54.3	309	58.4	144.2	16.46	83.6	11.13
Big_Ridge_M1_4	895	720	829	1515	16	5.4	835	2094	343	1811	445	23.9	447	61.3	340	61.2	152.6	18.1	91.2	11.55
Big_Ridge_M1_5	1000	566	748	926	20.2	4.1	715	1822	296	1542	339	23.1	328	42.7	234	42.6	104.3	11.66	60.2	8.38
Big_Ridge_M1_6	817	570	725	1317	13.85	3.75	699	1746	301	1623	383	24.3	382	51.7	294	55.1	138.5	16.09	83.6	10.78
Big_Ridge_M1_7	1270	623	855	1653	20.3	10.66	824	2140	369	1992	509	24.3	502	68.5	391	71.2	174	19.6	99	12.76
Big_Ridge_M1_8	574	697	576	1493	29.9	4.51	869	2130	358	1920	452	28	429	57	321	57.9	146.2	16.6	85.9	11.49
Big_Ridge_M1_9	876	714	860	1494	15.72	4.32	804	1893	317	1680	404	23.8	394	55.1	317	57	142.6	16.41	84.2	10.76
Big_Ridge_M1_10	1014	596	812	1398	21.8	4.53	788	1967	340	1830	437	23.9	420	55.8	314	57.5	140.5	16.5	84.7	10.84
Big_Ridge_M1_11	842	665	817	1162	12.96	4.27	783	1892	316	1655	373	23.4	363	48.7	273	49.6	118.6	13.63	70.7	9.14
Big_Ridge_M1_12	1142	815	1081	1766	27.5	3.95	869	2095	365	2017	477	24.56	468	63.2	377	74.8	204.2	25.5	138.8	18.79
Big_Ridge_M1_13	396	614	574	1669	26.5	3.93	932	2289	385	2116	508	29	502	66.8	374	67	164.9	18.36	93.1	11.84
Big_Ridge_M1_14	916	689	841	1641	15.97	5.85	807	1915	329	1744	438	21.8	460	64.8	369	68.7	167.3	18.12	91	11.83
Big_Ridge_M1_15	447	577.7	613	2162	105.1	23.4	1276	3030	507	2760	649	37	636	85.6	474	85	207.8	23.8	120.2	15.8
Big_Ridge_M1_16	994	753	1006	2099	11.68	7.75	659	1743	308	1730	486	21.25	537	78.5	463	88.5	218.9	24.9	124.2	16.47
Big_Ridge_M1_17	273	764	509	1867	31.9	4.08	539	1427	265.8	1544	454	26.31	490	69.5	405	74.8	185	21.3	109.2	14.14
Big_Ridge_M1_18	838	710	859	2630	39.1	8.99	997	2485	431	2320	618	27.2	662	99.3	585	110.3	273	30.5	153.7	19.5
Big_Ridge_M1_19	873	693	831	1497	14.7	5.07	773	1850	313.4	1644	396	21.38	405	56.5	319	57.6	143	15.9	79.9	10.23
Big_Ridge_M1_20	1110	580	822	1415	22	4.39	745	1822	316	1720	416	27.8	412	55.5	318	58.7	145.2	16.5	85.3	11.05
Big_Ridge_M1_21	862	528	737	1599	17.6	8.33	717	1778	315	1721	450	23.9	475	67.2	395	72.3	177	19.5	94.2	12.34
Big_Ridge_M1_22	1193	548	807	1283	17.1	4.28	775	1796	307	1697	390	23.6	378	50.3	278	49.4	123.4	14.1	70.1	9.17
Big_Ridge_M1_23	928	502	742	1468	23.3	4.84	793	1897	328	1810	436	26.5	435	59.1	325	57	140.4	16.2	82.5	10.75
Big_Ridge_M1_24	752	695	797	1486	21.8	4.65	691	1820	317.7	1757	460	22.78	452	62	353	63.6	157.7	17.51	89.3	11.75
Big_Ridge_M1_25	824	690	816	1490	19.7	5.29	821	2029	339	1818	434	25.6	427	58.8	334	60.9	150.3	16.94	87	11.28
Big_Ridge_M1_26	309	554	613	1319	14.1	3.7	743	1840	302	1549	373	26.3	385	52.3	295	54.7	134.3	14.99	74.5	9.62
Big_Ridge_M1_27	188	763	449	1888	37.5	6.39	545	1435	269.3	1584	473	27.6	505	72.7	416	76.2	188.2	21.67	109.3	14.04
Big_Ridge_M1_28	230	762	480	1383	19.2	3.33	439	1271	226	1228	344	20	353	50.3	292	52.7	132	15.1	81.2	10.67
Big_Ridge_M1_29	374	748	630	1263	23.8	4.7	812	2070	334	1677	368	23.6	336	45.3	250	46.2	121.5	14.95	81.6	11.26
Big_Ridge_M1_30	908	681	840	1657	13.47	4.93	761	1792	305.3	1662	428	19.71	454	65.3	377	68.7	168.7	18.58	91.9	11.95
Big_Ridge_M1_31	1061	819	1080	1450	14.2	4.35	665	1760	305	1610	407	21.1	417	59	330	58.5	146	17.6	90.6	11.6
Big_Ridge_M1_32	822	694	816	1376	11.8	4.85	674	1712	291	1552	386	21.7	388	54.1	315	57.6	140.8	15.66	77.9	10.16
Big_Ridge_M1_33	769	677	803	541	18.4	5.14	666	1526	226	1022	182	23.4	154.2	19	97.7	17.4	47.1	5.76	31.5	4.57

Table A1. Cont.

Sample Name	Mg	Mn	Fe	Y	Th	U	La	Ce	Pr	Nd	Sm	Eu	Gd	Tb	Dy	Ho	Er	Tm	Yb	Lu
Big_Ridge_M1_34	961	730	893	1255	13.7	3.43	706	1780	304	1620	388	23.2	384	50.8	283	51.2	126.3	13.9	69.3	9.27
Big_Ridge_M1_35	853	667	821	1798	21.3	8.75	796	1942	350	1917	490	24.8	488	68.5	399	74	186	20.9	106.8	13.52
Big_Ridge_M1_36	1070	768	582	1450	15	3.41	444	1200	225	1273	376	21.9	397	57.7	324	60.5	152	17	85	10.67
Big_Ridge_M1_37	854	504	721	807	14.09	3.49	573	1383	229	1166	257	22.28	232	30.8	170.1	30.8	76.4	8.98	47.5	6.44
Big_Ridge_M1_38	1059	615	959	1765	57.3	16.3	925	2310	396	2120	518	25.4	505	70.3	413	73.8	187	22.2	118	16.6
Big_Ridge_M1_39	188	741	430	1376	19.1	2.98	509	1310	238	1321	354	20.8	356	50.2	296	53.4	133.6	15.2	81.6	10.64
Big_Ridge_M1_40	830	892	1019	2052	19.67	5.33	656	1657	301.2	1683	464	23.37	484	72.1	425	79.7	205.2	23.98	123.9	16.39
Big_Ridge_M1_41	774.2	650	795	1337	18.46	4.59	774	1786	309.7	1701	398	22.21	388	52.4	295.9	54	137	15.56	80.5	10.39
Big_Ridge_M2_1	839	584	828	621	25.6	8.12	655	1581	235	1085	209.6	24.9	179.6	23.5	124.8	22	59.3	7.68	41.3	5.83
Big_Ridge_M2_2	1160	1028	1419	1853	18	8.53	519	1487	263.1	1424	419	20.54	460	70.1	416	75.8	196.8	24	117	15.08
Big_Ridge_M2_3	508	831	820	1245	14.76	3.6	509	1407	248.1	1302	350	20.48	342	49.2	277	48	122.8	14.72	73.3	9.6
Big_Ridge_M2_4	998	508	973	1112	21.2	4.28	742	1695	292.3	1628	369	26.49	357	46.4	253.8	45.4	116.1	13.6	67.9	9.32
Big_Ridge_M2_5	990	915	1248	1843	11.69	5.5	486	1456	245	1306	376	17.49	414	65.3	391	72	191	23.2	116.5	15.2
Big_Ridge_M2_6	782	792	1086	1720	13.2	4.75	533	1496	263	1392	384	18.2	411	61.3	354	65.2	172	20.5	99	13.03
Big_Ridge_M2_7	1160	694	656	1386	25.1	3.22	477	1226	219	1245	346	20.9	350	50.1	283	51	127.7	15.28	76.1	9.91
Big_Ridge_M2_8	693	550	771	1358	18.9	3.34	670	1669	283.1	1515	383	20.59	379	54	298	52.2	133.9	15.49	74.7	9.79
Big_Ridge_M2_9	709	459	752	800	14.84	4.44	714	1790	280	1379	282	21.99	256	33.6	182	31.9	81.6	9.51	47.1	6.36
Big_Ridge_M2_10	1260	508	841	1002	15.1	6.22	579	1622	257	1249	310	21.6	312	43	240	42	105.9	11.69	57.5	7.37
Big_Ridge_M2_11	628	743	934	1091	16.3	6.26	622	1746	294	1480	382	21.33	367	49.6	269	46.7	113.6	12.78	61.8	8.18
Big_Ridge_M2_12	229	724	477	1599	16.4	3.98	525	1499	264	1427	409	24.3	413	60.9	348	60.8	151.3	17.88	87.7	11.36
Big_Ridge_M2_13	761	636	888	1637	18.33	6.98	689	1839	314	1685	439	21.2	450	64.4	373	69.1	174.4	20.64	101.9	13.51
Big_Ridge_M2_14	783	640	822	1048	14.9	4.02	627	1573	254.4	1319	315	22.1	308	42.4	235	42.2	105.4	12.48	61	8.09
Big_Ridge_M2_15	139.2	819	438	1088	10.84	1.85	373	1039	182	967	265	15.8	276	39.3	226	40.4	100.1	11.88	58	7.61
Big_Ridge_M2_16	733	570	869	794	15.98	3.67	783	1955	301	1497	293	21.4	256	32.5	172.1	29.7	77.7	9.23	47.4	6.54
Big_Ridge_M2_17	1165	872	1395	1985	10.35	4.35	493	1399	246.3	1323	387	17.01	428	66.8	404	75.9	195	23.66	117.2	15.1
Big_Ridge_M2_18	1059	823	1330	1770	14.41	5.48	596	1651	289	1514	417	19.87	434	64.3	378	68.9	180.2	21.2	102.5	13.61
Big_Ridge_M2_19	766	803	1046	1615	13.72	6.04	676	1812	309	1631	415	19.12	422	60.5	347	63.2	160.2	18.97	94.6	12.56
Big_Ridge_M2_20	823	712	1001	1462	11.19	3.65	564	1563	268	1433	378	18.6	377	54.4	321	58.6	151.7	18.2	88.4	11.43
Big_Ridge_M2_21	382	931	512	1018	25.4	2.89	806	1866	277	1282	263	17.51	235.7	32.2	181.7	34.2	94.5	12.68	69.5	9.59
Big_Ridge_M2_22	991	575	965	1049	7.84	2.98	609	1559	249.3	1326	313	18.11	309	42	238	41.6	104.4	12.25	60.1	7.82
Big_Ridge_M2_23	1148	688	1168	1759	34.8	4.31	622	1603	288	1637	457	24.7	465	68.4	398	71.6	184	22.2	110.5	14.6
Big_Ridge_M2_24	1099	461.5	830	613	16.6	4.25	713	1739	262	1222	234	21.63	196.1	24.7	130.7	23.2	60	7.53	40	5.51
Big_Ridge_M2_25	868	939	1188	2192	22.7	5.64	608	1676	296.7	1638	471	22.42	489	74.6	450	83.9	223.4	27.6	138.3	18.43
Big_Ridge_M2_26	769	787	1090	1437	17.7	5.43	571	1454	257	1433	395	18.83	396	57.1	313	53.9	134.2	15.51	74.9	10.38
Big_Ridge_M2_27	690	540	812	902	14.38	3.77	689	1624	268	1376	309	23.8	285	37.5	204	35.2	88.4	10.35	51.4	6.88
Big_Ridge_M2_28	896	483	921	1166	14.53	4.1	659	1670	276.4	1443	357	20.31	352	48.2	267.6	46.1	114.9	13.27	64.4	8.23
Big_Ridge_M2_29	704	687	926	1451	14.72	4.52	659	1730	288	1515	393	21.5	388	54.4	302	53.5	137.9	16.64	83.4	10.56

Table A1. Cont.

Sample Name	Mg	Mn	Fe	Y	Th	U	La	Ce	Pr	Nd	Sm	Eu	Gd	Tb	Dy	Ho	Er	Tm	Yb	Lu
Big_Ridge_M2_30	1470	712	1113	2083	30.4	5.86	587	1500	263	1468	431	20.1	469	73.3	453	84	222	26.9	136.1	17.4
Big_Ridge_M2_31	972	683	1149	1458	11.13	4.03	589	1569	264	1415	376	17.61	387	56.1	327	58.2	146.5	17.3	82.8	10.66
Big_Ridge_M2_32	745	659	846	926	14.4	5.39	655	1619	254	1273	298	19.84	290	38.6	216	38.9	95.3	10.83	53.1	6.95
Big_Ridge_M2_33	963	714	1030	1446	15.75	4.22	799	2076	344	1800	436	22.8	415	57.7	322	58.1	147.2	16.9	83.3	10.83
Big_Ridge_M2_34	1071	829	1180	1961	15.7	4.39	545	1462	258	1434	427	18.54	455	71.7	430	78.6	204	24.5	123.6	16.23
Big_Ridge_M2_35	725	474	759	1013	14.29	3.68	682	1699	270.3	1413	317.9	21.93	297.8	41.2	225.2	39	98.8	11.6	58	7.65
Big_Ridge_M2_36	176.6	732	458	1439	15	3.16	511	1422	247	1326	368	21.8	379	54.7	311	54.9	138.5	15.94	78.3	10.29
Big_Ridge_M2_37	981	708	1151	1918	17.3	4.48	661	1708	299	1666	453	21.05	475	70.4	415	75.2	190.2	22.8	113.5	14.95
Big_Ridge_M2_38	167.3	704	453	1547	23.3	3.24	465	1234	220.1	1266	377	21.68	392	57.3	331.6	59.4	147.9	17.46	86.7	11.1
Big_Ridge_M2_39	835	530	889	831	12.83	3.36	684	1675	260	1297	279	20.94	256	34.1	183	32.6	82.9	9.71	49.3	6.66
Big_Ridge_M2_40	1295	726	1127	1558	24.4	5	543	1438	251	1384	402	22.6	418	62.7	358	64.3	162	19.1	93.5	11.96
Big_Ridge_M2_41	717	583	841	1110	13.4	4.15	637	1688	276	1437	354	21.4	350	47.7	266	47.2	117.4	12.9	63.1	8.14
Big_Ridge_M2_42	850	540	804	961	18.2	3.91	780	1859	293	1447	314	23.7	283	36.9	200.3	34.3	85.9	10.28	54.3	7.25
Big_Ridge_M2_43	816	672	903	1113	11.27	4.09	641	1590	256.2	1314	325	20.14	319	44.5	256	46.7	115.6	13.21	65.6	8.38
Big_Ridge_M3_1	203	748	517	812	15.7	1.91	509	1380	224	1130	259	18.9	227	27.8	153	26.9	66.8	8.08	42.7	5.55
Big_Ridge_M3_2	214	844	433	1800	31.2	3.94	429	1177	224	1293	406	20.8	436	64.5	374	68.6	173	19.4	99.4	12.85
Big_Ridge_M3_3	148	857	431	2210	36.8	5.44	494	1326	255	1544	500	23	536	78.5	464	86.4	216	24.7	127	15.9
Big_Ridge_M3_4	191.2	860	443	1881	26.3	3.58	458	1209	234	1376	432	22.1	460	67.9	400	73.5	182	21	104.3	13.66
Big_Ridge_M3_5	222	657	520	1303	50.7	3.54	595	1530	267	1440	365	24.8	349	47.8	265	46.3	116	13.67	75.9	10.15
Big_Ridge_M3_6	189.8	762	456	1229	11.16	2.27	403	1098	196.6	1071	304	17.7	309	43.7	253	45.4	117.8	14.05	70.2	9.18
Big_Ridge_M3_7	241	725	492	1032	12.6	6.24	358	1007	179	988	285	14.74	302	42.8	232	40.2	100.3	10.82	56.2	7.24
Big_Ridge_M3_8	285	849	483	2440	62.9	5.9	713	1799	342	2029	599	33.1	627	89.7	519	93.4	235	26.8	136	17.6
Big_Ridge_M3_9	284	730	449	1190	33.1	2.06	422	1111	198.5	1099	303	19.7	303	42.4	242	43.4	110.9	12.6	63.8	8.05
Big_Ridge_M3_10	244	680.3	435	1431	66.5	2.69	466	1123	217.9	1262	369.8	24.1	379	54.4	309	54.5	135.8	15.3	78.3	10.24
Big_Ridge_M3_11	198.5	724	455	1011	24.7	2.46	460	1260	211.4	1115	287	20.79	279	38.9	216.7	38.9	98.9	11.08	57.5	7.31
Big_Ridge_M3_12	164	746	447	1789	8.35	8.08	437	1259	234	1289	400	23.9	448	68.9	404	74.9	182.2	20.4	100.5	12.68
Big_Ridge_M3_13	169.4	875	447	2220	31.5	6.34	623	1729	316	1820	530	26.8	541	78.1	458	82.2	212	24.5	128	16
Big_Ridge_M3_14	261	750	483	1548	17.5	7.52	588	1619	283	1545	399	23.9	404	58.1	333	59.4	150.8	17.19	88.3	11.34
Big_Ridge_M3_15	158	885	432	1522	14.45	3.14	446	1264	227	1256	361	18.93	354	52.1	307	55.3	142.9	16.54	84.9	10.93
Big_Ridge_M3_16	280	678	516	1071	11.34	2.6	627	1594	272.2	1430	332.3	20.26	308	41.7	231.8	41.7	105.5	12.31	64.1	8.21
Big_Ridge_M3_17	199.6	755	454	1656	26	3.95	469	1284	240	1383	419	24.9	430	62.4	365	66.2	166.8	18.88	95.1	12.3
Big_Ridge_M3_18	316	707	456	1375	50.7	3.08	399	1082	202.9	1149	343	21.7	363	51.7	294	53.4	133.9	15.21	75.7	9.7
Big_Ridge_M3_19	498	425	593	1463	20.1	3.65	798	1941	331	1801	451	25.5	428	57.7	317	57.6	140.8	15.65	80	10.11
Big_Ridge_M3_20	159.4	872	419	1580	21.7	3.17	521	1310	244	1460	425	21.3	432	59	338	64.5	157.2	18.1	91.7	11.31
Big_Ridge_M3_21	355	742	508	1430	14.6	3.47	440	1214	225	1281	366	21.2	377	52.8	301	55.5	140.4	15.5	79.1	10.07
Big_Ridge_M3_22	312	734	575	1063	19.7	4.53	656	1723	293	1465	332	21.5	296	39.7	220	39.4	106.6	12.09	66.8	8.68

Table A1. Cont.

Sample Name	Mg	Mn	Fe	Y	Th	U	La	Ce	Pr	Nd	Sm	Eu	Gd	Tb	Dy	Ho	Er	Tm	Yb	Lu
Big_Ridge_M3_23	169.2	912	436	1660	21.6	3.35	445	1234	226	1266	383	18.4	403	59.2	343	63	160	18.1	90.7	11.39
Big_Ridge_M3_24	219	822	550	1690	49.5	4.45	421	1174	224	1330	419	22.7	434	62.4	356	64.1	158.6	18.1	95.1	12.39
Big_Ridge_M3_25	213	741	459	1718	30.1	7.53	503	1444	268	1519	444	24.4	435	63	362	65.8	170	19.63	100.2	13.02
Big_Ridge_M3_26	858	832	534	1288	16.8	2.67	413	1151	207.6	1151	325	16.49	310	46	268	48.2	126.2	14.41	76	9.71
Big_Ridge_M3_27	153	846	570	1212	14.13	2.54	456	1237	217	1159	305	16.71	293	41.9	245	44	112.8	13.74	70.9	9
Big_Ridge_M3_28	154.1	807	444	1850	18.8	4.34	555	1489	271	1555	454	25.1	464	68.5	393	69.4	179	20.8	106.2	13.64
Big_Ridge_M3_29	287	755	488	1867	28.8	5.26	550	1521	286	1618	469	26.8	477	68.9	396	71.5	183.5	21.17	109.4	13.99
Big_Ridge_M3_30	190	740	459	1178	16.8	3.06	438	1197	213.7	1176	317	20	307	43.2	249	44.6	113.3	13.04	68	8.9
Big_Ridge_M3_31	180.7	746	446	1660	41.7	8.3	465	1309	246	1415	432	25.4	427	61.8	351	63.9	166.3	19.47	98.5	13.09
Big_Ridge_M3_32	148	871	464	2110	26.8	5.55	496	1376	262	1530	483	23.7	513	73.9	432	77.8	197	22.8	116	14.3
Big_Ridge_M3_33	172	875	455	1865	34.4	4.1	539	1491	270	1521	440	23.3	454	65.7	383	69.7	177.4	20.32	105.1	13.45
Big_Ridge_M3_34	336	643	602	946	20.3	3.38	729	1670	278	1426	308	20.3	272	35.6	197	36.1	94.2	11.01	59.1	8.28
Big_Ridge_M3_35	165.3	697	440	1657	47.4	3.5	539	1446	266	1528	433	25	438	62.7	358	64.6	167	18.29	92.6	11.77
Big_Ridge_M3_36	358	527	606	1215	11.9	3.28	709	1641	286	1579	381	21.56	375	49.2	271	48	120.2	13.38	66.6	8.25
Big_Ridge_M3_37	284	817	467	1940	69.6	4.3	633	1609	297	1745	498	28.7	504	71.6	401	71.4	181	20.8	106.3	13.9
Big_Ridge_M3_38	185	945	430	1485	23.5	2.48	443	1100	210	1246	351	18.4	367	50.6	297	53	135	15.6	82.5	10.64
Big_Ridge_M3_39	308	541	596	1035	23.2	5.69	608	1545	262	1390	332	19.76	305	41.1	225	40.8	101.1	11.05	57	7.42
Big_Ridge_M3_40	136.8	840	427	1581	30.6	2.98	391	1020	195.2	1168	367	18.8	391	56.3	329	59.9	151.1	17.3	87.1	11.2
Big_Ridge_M3_41	170.9	812	435	2520	90	6.22	594	1645	314	1876	594	31.4	625	92.2	533	95.5	248	27.9	143.8	18.2
Big_Ridge_M3_42	173.8	740	454	1550	16.3	4.35	484	1430	258	1410	393	22.4	395	55.4	318	57.8	149	17.7	89.3	11.34
Big_Ridge_M3_43	165.9	788	469	1660	15.1	3.77	549	1601	284	1557	429	24.7	431	61.2	355	61.1	156	18.2	92.5	11.92
Big_Ridge_M3_44	162	875	451	1150	9.66	2.31	481	1320	224	1100	275	15.3	273	41.1	226	39.3	101	11.9	61.8	8.31
Big_Ridge_M3_45	171.4	753	496	1656	16.7	3.79	518	1449	263	1464	425	24.9	418	58.7	344	62	161	17.92	93.7	11.71
Big_Ridge_M4_1	138.7	881	1570	1170	10.02	2.78	463	1438	229	1158	310	17.24	300	43.1	247	44	112.8	13.25	64.7	8.28
Big_Ridge_M4_2	290.6	512	624	1189	17.4	3.02	676	1678	271	1440	347	21.62	324	46	263	47.7	119.6	13.81	71.1	9.21
Big_Ridge_M4_3	505	741	540	1194	15	3.24	466	1420	229.6	1159	326	20.61	321	46.4	266	47.8	115.3	13.48	66.7	8.68
Big_Ridge_M4_4	363	694	516	1373	27.2	2.77	508	1243	217.8	1239	351	21.31	361	51.2	295	52.5	126.6	14.75	72.1	9.33
Big_Ridge_M4_5	342	771	529	1511	32.2	4.83	461	1428	238	1278	378	22.8	390	56.8	332	59.5	145.8	16.82	86.3	11.05
Big_Ridge_M4_6	970	759	667	1628	30.4	5.55	608	1826	304	1615	447	27.5	432	64	366	63.7	163.5	19.1	94.9	11.82
Big_Ridge_M4_7	335	702	483	1395	41	4.12	502	1306	225.1	1268	360	22.27	366	53.4	311	55.5	136.4	15.92	80	10.26
Big_Ridge_M4_8	367	565	645	869	20.7	4.85	530	1499	228	1133	263.8	15.06	242.9	33.2	188.4	33.7	83.6	9.81	49.8	6.58
Big_Ridge_M4_9	355	565	694	1009	31	2.73	634	1810	275	1356	323	21.1	299	40.9	229	41	101.5	11.26	55.6	7.11
Big_Ridge_M4_10	430	787	670	1154	15.7	2.66	406	1245	202.5	1045	286	17.93	292	41.6	247	43.2	109.6	12.68	64.2	8.17
Big_Ridge_M4_11	241	847	456	2110	43.1	5.68	603	1616	284	1610	484	26.2	519	78.5	457	81.6	210	24.1	122.5	15.9
Big_Ridge_M4_12	278	854	706	1082	20.5	6.43	709	2360	333	1440	333	24.6	307	42.8	241	42.8	108	13.03	71.5	9.2
Big_Ridge_M4_13	195	746	659	909	6.41	5.37	390	1073	172.8	902	242	14.84	252	36.5	209.5	37	91.2	10.07	49.2	6.23

Table A1. Cont.

Sample Name	Mg	Mn	Fe	Y	Th	U	La	Ce	Pr	Nd	Sm	Eu	Gd	Tb	Dy	Ho	Er	Tm	Yb	Lu
Big_Ridge_M4_14	368	756	536	747	9.5	1.77	349	1112	171	803	209	13.5	196	27.3	155	28.7	71.2	8.12	41.9	5.39
Big_Ridge_M4_15	398	800	537	865	29.5	2.04	372	1281	184	927	252	18.39	237	33.8	191.4	32.9	81.6	9.48	46.9	5.92
Big_Ridge_M4_16	344	705	515	1698	23.8	3.71	478	1285	226	1306	410	23.3	425	64.1	377	68.2	167	19.1	92.2	12.37
Big_Ridge_M4_17	410	608	744	1489	24.9	4.77	904	2820	408	1923	468	29.2	445	61	349	59.9	145.4	16.66	81.9	10.29
Big_Ridge_M4_18	637	831	589	1220	27.3	15.5	359	1220	192	983	292	18.7	301	45.7	276	50.9	127.2	14.4	74.7	9
Big_Ridge_M4_19	327	608	757	1369	16.9	4.54	877	2780	396	1830	431	25.7	395	57	310	54.5	134.3	14.8	74	9.37
Big_Ridge_M4_20	590	719	536	2430	61	7.2	628	1704	306	1800	573	33.2	607	91.7	523	94.4	233	27.6	142	18.6
Big_Ridge_M4_21	388	771	622	1540	48	3.4	507	1640	263	1370	398	26.9	409	60.1	343	60.3	144	16.7	80.8	10.2
Big_Ridge_M4_22	254	734	508	1810	33.3	3.89	591	1530	263	1550	458	30.1	430	63.1	372	68.3	157	18	90	12.7
Big_Ridge_M4_23	381	527	690	1244	25.4	3.82	908	2150	337	1663	364	22.4	328	44.7	252	46.1	117.6	13.64	70.7	9.39
Big_Ridge_M4_24	319	575	673	1750	31.2	5.99	950	2490	385	1930	488	29.2	514	73	392	73	175	19.7	99	13.1
Big_Ridge_M4_25	297	772	548	2010	45.2	8.1	615	2070	334	1720	511	30.7	525	76.1	424	75.4	189	22.3	107	13.8
Big_Ridge_M4_1	241	842	644	631	5.75	2.17	413	1390	204	858	188	13.6	161	21.4	118.6	22.3	52.9	6.31	32	4.25
Big_Ridge_M4_2	544	531	804	666	6.36	18.4	481	1701	240.1	989	218.1	15.02	212	29.2	157.1	26.3	56.9	5.94	29.1	3.62
Big_Ridge_M4_3	344	870	657	920	17.6	1.86	425	1530	223	1072	254	20.7	239	33.6	189	36.3	83.5	9.8	50.3	6.31
Big_Ridge_M4_4	750	925	716	1115	37.8	3.37	483	1854	287	1263	310	23.3	283	38.2	219	39.9	97.7	11.18	60	7.48
Big_Ridge_M4_5	208.2	917	624	1324	13.33	3.44	521	1906	294	1313	327	21.59	310	43.2	251.7	47	115.6	13.6	71.3	9.02
Big_Ridge_M4_6	238	887	586	1247	15.1	3.19	461	1677	263.3	1195	318	21.9	308	43.4	254	46.8	112.2	13.42	68.6	8.75
Big_Ridge_M4_7	243	738	558	1094	13.3	1.45	542	1440	249	1264	301	21.5	294	38.8	215	40.3	99.7	11.42	57.9	7.33
Big_Ridge_M4_8	275	803	605	960	8.72	1.332	350	1119	185	897	232	15.98	221.1	31.1	179.7	33.6	80.6	9.57	49.5	6.35
Big_Ridge_M4_9	309	822	626	1240	24	2.49	412	1337	223	1105	299	21.9	309	43.9	249	44.8	109.5	12.7	66.7	8.44
Big_Ridge_M4_10	364	807	588	2320	37.1	5.52	804	2320	399	2100	577	36.2	554	77.2	466	88.6	210	25	138	16.8
Big_Ridge_M4_11	230	855	490	1970	32.3	3.17	540	1510	279	1510	444	23.8	463	65.7	378	72.1	183	20.9	106.4	13.5
Big_Ridge_M4_12	376	920	717	1043	49	2.8	615	2160	320	1334	296	23.2	267	35.4	205	38.2	95.2	11.83	64.5	8.29
Big_Ridge_M4_13	220	936	593	1355	19.3	17.7	349	1287	189	852	243	15.66	253	41.1	267	51.8	131.4	15.5	82.4	10.67
Big_Ridge_M4_14	258	945	569	1370	17.8	2.05	360	1120	197	1010	301	18.3	303	43.4	261	47.5	117	14.3	71.9	9.1
Big_Ridge_M4_15	246	886	614	1270	15.2	2.84	394	1450	228	1089	298	21.7	309	43.2	244	43.7	107	12.5	64.4	7.99
Big_Ridge_M4_16	203	728	505	1616	22.4	2.54	493	1327	248	1385	400	25.6	413	59.7	339	61.5	157	17.5	87.3	11.35
Big_Ridge_M4_17	318	900	652	1250	24.9	1.61	401	1240	196	1000	280	20	273	39	217	39.2	97	11.5	57.5	7.94
Big_Ridge_M4_18	264	873	625	1530	40.3	6.1	523	1950	315	1380	381	25.2	406	58.5	310	58	140	17.1	86	10.9
Big_Ridge_M4_19	291	709	614	1340	45.9	1.92	608	1660	281	1399	345	25.1	345	47.1	257	47.4	121	13.9	70.1	9
Big_Ridge_M4_20	215	721	511	1670	25	3.81	529	1620	267	1360	382	26.4	384	56.3	349	61.1	148	18.1	90	12
Big_Ridge_M4_21	379	864	643	1560	19.7	3.24	591	2240	339	1520	373	24.3	353	52.6	307	58.5	145	16.9	85.9	11.2
Big_Ridge_M4_22	198	846	571	1042	12.3	2.21	399	1386	221	1010	259	19.4	257	35.8	200	36.2	90.5	10.29	53	6.74
Big_Ridge_M4_23	296	855	587	1224	12.19	2.44	477	1550	256	1225	316	22.6	306	42.7	242	44.5	106.3	12.35	64.3	8.05
Big_Ridge_M4_24	243	846	602	778	29.1	1.48	491	1560	231	1049	233	19.7	218	29.7	156	27.8	70.7	7.98	40.4	5.47

Table A1. Cont.

Sample Name	Mg	Mn	Fe	Y	Th	U	La	Ce	Pr	Nd	Sm	Eu	Gd	Tb	Dy	Ho	Er	Tm	Yb	Lu
BR0417_D1_1	843	460.9	772	1180	19.47	6.53	1011	3165	420	1805	371.9	28.51	345.1	45.5	253.5	46.7	116.9	13.39	68.7	8.85
BR0417_D1_2	855	445.6	743	1030	17	3.52	866	2679	361	1549	322	25.76	298.9	39.1	219.6	40.4	101.5	11.47	59.3	7.58
BR0417_D1_3	801	442.3	772	764	9.13	2.03	672	2002	273.3	1185	247.4	19.98	225.6	29.48	165.1	30.2	75.5	8.54	43.9	5.62
BR0417_D1_4	869	465	792	1268	26.9	5.5	1145	3490	465	1974	404	30.9	366	47.4	267.6	48.9	124.5	14.32	74.7	9.62
BR0417_D1_5	707	503	825	781	15.5	3.99	1001	2900	358	1419	260	19.1	231	28.5	159	29.9	77.4	9.17	49	6.54
BR0417_D1_6	820	452.9	820	717	9.04	2.47	729	2147	284.3	1210	239.8	18.52	214.6	27.3	153.2	28.28	71.9	8.22	42.4	5.43
BR0417_D1_7	796	445	729	703	9.6	1.96	670	2010	263	1102	219	17.5	201	26.1	144.7	26.7	67.3	7.73	40.4	5.2
BR0417_D1_8	774	423.6	704	580	5.12	2.85	561	1629	218.5	923	186.6	14.84	171.3	21.82	122.4	22.4	55.7	6.24	31.9	4.121
BR0417_D1_9	751	487.6	753	954	12.83	3.15	938	2763	366.8	1534	305.9	23.68	283.5	35.73	202.2	37.24	93.9	10.77	56.1	7.31
BR0417_D1_10	818	454.5	751	1207	21.8	4.85	1022	3110	421	1810	379	28.9	345	45.5	256	46.9	118.3	13.49	69.2	8.88
BR0417_D1_11	893	464.6	719	526	5.16	1.35	607	1797	226.4	913	173.4	13.65	153.1	19.45	107	19.67	49.9	5.71	30.1	3.97
BR0417_D1_12	734	483.7	725	938	18.3	3.94	1183	3379	424	1681	304.8	23.01	269.9	33.9	189.7	35.2	91.5	11.01	59	7.86
BR0417_D1_13	750	438.2	801	528.8	3.88	1.084	555	1585	209.6	880	171.1	13.83	157.9	19.66	109.1	20.09	50.5	5.79	29.82	3.9
BR0417_D1_14	689	520	751	1039	31.6	6.06	1406	4130	502	1937	337	25.8	296	36.6	207.7	38.7	101.7	12.31	67.5	9.06
BR0417_D1_15	794	445.6	732	1064	14.9	3.22	940	2780	374	1639	336	26.3	309	39.5	223.5	40.7	102	11.83	60.4	7.79
BR0417_D1_16	684	455.8	703	827	16.1	4.05	924	2690	346	1404	266	20.3	239	29.7	167	31.1	79.8	9.44	50.1	6.58
BR0417_D1_17	802	441.2	727	1199	24.1	4.68	1084	3240	434	1851	379	29	344	44.5	251	45.8	115.4	13.37	70.2	9.01
BR0417_D2_1	949	465	1377	453	2.36	0.973	465	1494	184.1	750	146.2	12.35	126.4	16.19	90.9	16.94	42.4	4.82	25	3.28
BR0417_D2_2	979	506	955	728	8.65	2.7	622	2280	268.3	1116	230.5	20.77	209.3	26.76	148.4	27.39	68	7.72	39.9	5.07
BR0417_D2_3	934	503	916	733	7.04	2.14	686	2424	307	1184	243.4	19.65	219.1	27.43	153.8	28.62	71.1	7.96	41.7	5.37
BR0417_D2_4	999	496	944	588	5.09	7	540	1842	229.7	940	189.3	16.41	177.9	22.5	125.6	22.8	57.1	6.36	32.5	4.22
BR0417_D2_5	945	494	923	872	12.4	10.9	713	2440	305.2	1267	257.9	21.73	232.5	30.08	172.6	32.6	86.1	11.02	66	9.2
BR0417_D2_6	842	483	1001	672	5.62	1.81	623	2159	266.9	1082	212.7	17.25	197.4	24.83	138.2	25.21	62.9	7.07	36.3	4.67
BR0417_D2_7	924	455	870	707	5.81	1.659	607	2061	260.5	1092	224.8	18.63	203	26.47	147.9	26.96	67.4	7.6	38.8	5.03
BR0417_D2_8	914	472	865	1039	16.1	4.96	861	2930	365	1581	322	26.7	300	38.8	218	39.5	97.8	11.34	58.5	7.41
BR0417_D2_9	894	442	850	548	2.89	1.032	490	1604	204.8	851	176.4	14.91	162	20.47	114	20.61	51.4	5.77	29.15	3.8
BR0417_D2_10	870	434	827	958	13.49	5.17	805	2430	329.7	1428	297	24	275	35.5	198.5	36.7	91	10.57	54.4	6.94
BR0417_D2_11	951	480	906	739	6.86	2.9	650	2217	275.2	1155	229.8	19.2	212.6	27.3	152	28.07	69.1	8.02	41.2	5.31
BR0417_D2_12	870	435	840	478	1.937	0.667	445	1430	181.3	754	149.6	12.54	140.5	17.52	97.4	17.73	44.4	4.95	25.37	3.32
BR0417_D2_13	827	478	895	546	3.81	2.48	555	1789	222.4	909	174.4	14.23	159.2	20	112.4	20.51	50.6	5.77	29.7	3.83
BR0417_D2_14	911	477	1021	781	7	2.044	691	2349	293.8	1216	240.2	19.54	219.9	28.74	159.1	29.53	73.2	8.36	42.5	5.51
BR0417_D2_15	980	481	953	610	6.11	1.804	524	1827	229.1	925	192	17.98	176.3	22.61	125.3	22.76	58	6.56	34.5	4.42
BR0417_D2_16	771	533	877	690	10.09	2.51	838	2890	329	1239	229.1	18.82	205	25.32	139	25.7	65.8	7.64	41.3	5.47
BR0417_D2_17	1037	528	1055	1303	27.2	10.1	1220	4360	524	2120	423	33.5	386	48.7	272	49.8	124.5	14.29	75.1	9.55
BR0417_D2_18	912	489	912	566	4.2	1.259	527	1851	216.6	910	183.4	15.27	164.1	20.73	117.8	21.74	53.1	6.01	30.5	3.99
BR0417_D2_19	1025	510	999	638	6.11	1.737	581	2126	251.4	1037	203.6	17.72	186.5	23.83	132.1	24.19	61.1	6.97	36.1	4.65
BR0417_D2_20	970	483	967	796	7.57	2.21	700	2434	299	1248	253.5	21.58	234.5	30.01	169.2	31.05	77.6	8.74	44.3	5.77

Table A1. Cont.

Sample Name	Mg	Mn	Fe	Y	Th	U	La	Ce	Pr	Nd	Sm	Eu	Gd	Tb	Dy	Ho	Er	Tm	Yb	Lu
BR0417_D3_1	811	474.5	925	934	18.7	4.41	989	3090	386	1558	295	23.8	260	33.3	187	34.4	87.8	10.32	54.6	7.19
BR0417_D3_2	795	461	780	816	11.48	2.43	761	2420	310	1292	260	20.43	237	30.7	170.1	31.5	79.8	9.14	47.3	6.11
BR0417_D3_3	1350	445.4	939	830	11.25	2.95	699	2261	288.8	1238	254.3	23.95	232.9	30.37	170	30.9	77.4	8.75	45.6	5.91
BR0417_D3_4	743	454.1	780	798	18.1	3.44	768	2440	309	1269	252	21.1	227	29.5	163	29.7	74.9	8.67	45.3	5.88
BR0417_D3_5	946	413.1	1003	598	7.74	2.197	456	1442	194.2	850	182.2	24.4	165.6	21.61	121.1	21.93	54.5	6.26	32.7	4.31
BR0417_D3_6	865	467.5	826	999	13.8	3.3	856	2770	359	1513	311	24.4	286	36.7	207.7	37.7	94.2	10.74	55.7	7.27
BR0417_D3_7	838	465.4	824	945	16.7	5.17	965	3050	378	1538	302	22.9	267	33.8	186.5	34.3	87.2	10.11	53.7	7.09
BR0417_D3_8	1305	562	1100	681	11.93	2.82	551	1685	228.8	992	211.8	25.04	188.5	24.21	134.3	24.57	60.4	7	37.4	4.91
BR0417_D3_9	1198	408.5	1029	704	8.98	2.57	554	1708	232.7	1043	219.5	25.16	211.6	27.23	150.7	27.5	68.9	7.74	40.2	5.19
BR0417_D3_10	1172	415	1011	636	8.39	2.16	532	1717	222.9	978	206.3	23.4	189	24.2	135.6	24.9	62	6.93	35.3	4.6
BR0417_D3_11	760	485	834	954	14.74	3.63	995	3140	397	1573	298	23.3	269.1	33.7	189.2	35.2	90.2	10.54	55.9	7.3
BR0417_D3_12	799	436.2	741	678	12.9	2.01	676	2048	267	1103	223.1	18.16	197.4	24.9	138.3	25.3	63.7	7.3	38.2	4.94
BR0417_D3_13	896	458.8	904	969	16.6	3.45	828	2700	347	1474	301	24.4	277	35.5	198	36.5	90.9	10.33	53.6	6.89
BR0417_D4_1	892	489	876	827	8.12	2.24	729	2470	308.2	1291	264.7	21.01	242	31.1	174.5	32	79	8.99	46.4	5.96
BR0417_D4_2	906	533	1290	653	5.32	1.801	635	2092	266	1062	217.6	18.54	195.7	24.24	135	24.91	62.4	7.06	36.1	4.75
BR0417_D4_3	662	592	891	676	11.36	3.95	907	2780	328.5	1269	224.1	14.61	195.6	24.16	133.6	25.04	65.4	7.91	42.4	5.71
BR0417_D4_4	809	483.2	856	808	10.48	2.52	718	2109	281.9	1232	246.6	20.68	228.6	29.39	163.7	30.16	76.1	8.77	45.9	6.01
BR0417_D4_5	779	418.2	770	1139	18.34	6.8	971	2772	385.8	1695	348.9	26.09	317.8	41.57	232.8	42.77	107.4	12.33	64	8.28
BR0417_D4_6	926	438.6	916	754	7.25	1.837	667	1965	266	1158	234.6	19.53	212.3	27.32	153.5	28.12	70.3	8.06	41.4	5.35
BR0417_D4_7	668	482	776	749	6.97	1.79	685	2050	274.7	1166	238	18.58	220.1	27.9	154.9	28.8	71.2	8.04	40.9	5.33
BR0417_D4_8	788	471	951	1085	22.2	4.68	1136	3490	441	1770	338	26.03	301.6	38.3	216.9	40.3	102.9	12.15	64.5	8.61
BR0417_D4_9	957	502	1131	1025	11.05	8.96	702	2360	295	1272	275.2	20.1	285.3	40.2	236	45	109.4	11.66	56.8	7.27
BR0417_D4_10	712	608	1183	557	6.31	1.712	698	2137	256.8	1003	181.9	14.7	164	19.73	109.5	20.38	52.6	6.26	33.8	4.55
BR0417_D4_11	779	437.9	779	625	4.12	1.118	581	1706	228	968	195.1	15.45	177.4	22.81	127.1	23.34	58.2	6.61	34.23	4.48
BR0417_D4_12	765	545	955	958	24.18	6.37	1268	3820	451	1775	310.2	23.25	269.4	33.69	187.6	35.05	91.7	11	61	8.16
BR0417_D4_13	813	463.4	856	626	5.3	1.37	585	1732	227.7	985	199.5	16.16	181.4	23.1	127.8	23.63	59.2	6.67	34.4	4.47
BR0417_D4_14	1020	385.5	989	739	9.44	2.582	561	1715	238.1	1075	232.2	23.22	215.9	28.14	155.9	28.41	70	7.85	39.7	5.13
BR0417_D4_15	891	419.3	836	710	9.05	2.037	767	2144	279.4	1176	224.5	17.88	207.7	25.76	144.3	26.75	67.9	7.94	41.5	5.5
BR0417_D4_16	716	448	760	493	2.04	13.41	494	1382	184.8	790	155.4	12.59	144.5	18.57	102.3	18.57	45.9	5.15	26.58	3.56
BR0417_D4_17	631	556	839	603	6.99	2.22	784	2174	274.7	1116	196.2	13.64	175	22.19	121.4	22.98	60.1	6.94	36.7	4.9
BR0417_D5_1	1022	436.3	844	788	14.43	2.9	668.2	2047	275.3	1189	247.8	21.14	226.1	29.13	164.4	30.17	75.7	8.64	44.9	5.69
BR0417_D5_2	771	442	690	542.2	3.18	1.028	543.7	1637	215.1	890	177.1	14.11	160.1	20.24	113.2	20.79	51.9	5.88	30.05	3.9
BR0417_D5_3	822	429.6	727	730	6.67	1.706	639	1937	257	1107	227.1	18.65	208	26.95	151.8	27.76	70.1	7.85	40.7	5.23
BR0417_D5_4	837	459.9	785	953	15.3	2.95	812	2545	338.1	1448	299.5	22.76	278.4	36	202.5	36.7	91.3	10.39	53.3	6.72
BR0417_D5_5	906	466.1	790	681	9.28	2.312	597.1	1879	246	1026	215.8	18.9	193.7	25.1	142	26.01	64.8	7.51	38.9	4.96
BR0417_D5_6	839	449	720	1194	21.5	3.73	966	2920	394	1750	371	29.6	347	45.1	253	46.1	116.6	13.3	69.2	8.84

Table A1. Cont.

Sample Name	Mg	Mn	Fe	Y	Th	U	La	Ce	Pr	Nd	Sm	Eu	Gd	Tb	Dy	Ho	Er	Tm	Yb	Lu
BR0417_D5_7	959	501.2	793	488	10.85	2.73	693	2063	249.8	983	177.7	23.09	152.5	18.51	101	18.48	48.1	5.65	31.2	4.27
BR0417_D5_8	716	376.6	658	1435	28.1	4.98	1109	2460	391.1	1955	422.6	31.96	397.3	52.3	298.1	54.4	136.2	15.61	79.8	10.26
BR0417_D5_9	879	470.9	781	1674	43.3	8.79	1317	4230	572	2450	528	41.1	484	64.7	360	66.3	165.2	18.9	97.2	12.37
BR0417_D5_10	900	462	787	1008	14.32	5.01	845	2719	355	1513	314.3	25.69	293.3	38.2	216.2	40	100.3	11.29	58.6	7.45
BR0417_D5_11	802	544	796	1205	23.5	5.32	1171	3690	466	1935	377	29	339	44	249.8	46	119	13.91	73.6	9.52
BR0417_D5_12	859	455.6	787	981	24.4	4.92	904	2770	363	1531	311	25.1	285	36.5	206	37.8	95.3	11.04	58	7.46
BR0417_D5_13	820	436.5	710	954	12.45	3.04	795	2477	331	1404	294.1	23.52	271.2	35.4	198.2	36.3	91	10.4	53	6.76
BR0417_D5_14	826	455	741	845	24.1	2.76	766	2320	310	1321	273	23.6	251	32.6	181	32.8	82	9.43	48.9	6.28
BR0417_D5_15	852	499	729	959	21.8	4.96	888	2700	353	1471	298	27.2	273	36.1	202	37.2	93.2	10.86	57.3	7.35
BR0417_D5_16	819	450.7	777	875	27.1	24.9	718	2159	283.4	1206	248.3	19.97	224.8	29.41	173.8	33.5	93.2	13.11	85.9	12.37
BR0417_D5_17	882	452.6	745	897	16	7.52	761	2375	314.5	1338	278.3	23.84	255.8	33.44	188.4	34.36	85.3	9.72	49.8	6.39
BR0417_D6_1	884	422.3	819	938	53.9	2.979	905	2051	299.8	1368	273.1	28	240.2	31.07	178.5	33.8	88	10.71	57.4	7.61
BR0417_D6_2	778	398.9	732	958	20.6	2.92	834	2152	305	1410	290.9	23.76	262.7	33.9	191.8	35.4	89	10.29	53.9	7.04
BR0417_D6_3	825	430	849	775	13.19	1.763	730	2000	271.3	1189	242.2	20.19	216.8	28.08	157.1	29.05	73.6	8.48	44.6	5.78
BR0417_D6_4	884	438	829	1226	17.77	5.3	966	3034	409	1763	358	29.2	342	44.1	253.1	46.2	116.2	13.47	69.3	8.86
BR0417_D6_5	811	463	807	750	8.81	2.21	727	2193	285.7	1211	236.4	19.09	217.9	27.3	154.2	27.91	69.7	8	41.9	5.47
BR0417_D6_6	1302	541	1893	635	9.53	3.32	505	1480	206.4	913	187.5	18.98	178	22.88	130.2	24	61.2	7	36.1	4.84
BR0417_D6_7	1143	431	1039	694	9	2.289	550	1716	229	996	217.4	23.77	199	25.98	143.9	26.19	64.9	7.42	38.1	4.95
BR0417_D7_1	800	490.6	853	885	21.32	3.41	692	2036	282.5	1246	269.6	27.91	247.3	32.2	182.1	33.3	84.8	9.7	49.8	6.46
BR0417_D7_2	947	421.5	763	1041	25.2	2.414	829	2361	327.6	1482	323.7	27.72	300.6	39.16	217.2	39.87	99.3	11.38	58.9	7.46
BR0417_D7_3	822	424.5	776	1012	24.83	3.39	803	2364	322.2	1432	301.8	24.68	283.8	37.12	208.1	38.17	95.3	10.9	56.6	7.24
BR0417_D7_4	815	453.5	845	635	7.55	2.308	674	2058	261.4	1072	206.8	16.74	180.3	22.95	127.7	23.29	59.3	6.83	36.03	4.71
BR0417_D7_5	831	415.6	780	1068	21.5	2.52	827	2267	322.7	1470	317.6	26.65	298.1	39.1	221.6	40.4	100.8	11.71	60.5	7.83
BR0417_D7_6	907	471.8	837	1214	29.7	3.31	985	2682	368.3	1709	364.3	25.18	346	44.82	251.3	45.85	114.8	13.18	68.9	8.9
BR0417_D7_7	967	427.3	786	710	5.95	1.433	600.2	1813	240.9	1066	220.7	17.97	206.6	25.87	146	26.65	66.1	7.43	38.36	4.97
BR0417_D7_8	811	422.4	740	804	9.85	1.965	710	2060	279.3	1226	249.8	20.5	232.1	29.95	168.3	31	77.8	8.81	45.2	5.88
BR0417_D7_9	855	441	798	1301	34.1	4.91	1085	3330	441	1899	397	32.5	357	47	266	48.8	123.1	14.46	75.3	9.62
BR0417_D7_10	794	466.8	802	1240	31.5	4.34	1130	3100	425	1883	379	31.4	346	44.7	251	46.5	119.1	14.02	74.4	9.8
BR0417_B1_1	2046	637	1083	566	9.2	1.92	421	1026	151.8	713	156.4	26.6	147.7	20.6	119.1	21.9	56.7	6.51	34.1	4.67
BR0417_B1_2	1941	616	1126	737	17.2	2.97	576	1363	199.1	953	210	26.7	192	25.9	146.9	26.9	68.4	7.99	41.8	5.69
BR0417_B1_3	1860	652	1052	558	37.4	2.17	438	1097	162	771	163	28.3	149	20.7	116	21.4	53.5	6.27	33.3	4.73
BR0417_B1_4	1588	719	1067	843	14.9	3.42	670	1641	235	1097	248	34.1	232	31.9	187	34.1	85.4	9.9	52.1	7.12
BR0417_B1_5	2092	544	1038	703	13.66	2.54	488	1002	159.3	858	199.9	31.9	190	26.2	152.6	28.1	70.7	8.12	41.8	5.63
BR0417_B1_6	1226	739	1006	1063	19	4.08	738	1760	261	1336	298	45.8	276	39.6	228	42.9	108	12.6	65.2	8.88
BR0417_B1_7	994	725	806	1389	61.2	4.98	1052	2610	371	1850	415	47.3	376	52.3	299	55.8	139	16.2	84.3	11.6
BR0417_B1_8	2357	592	1177	545	13.9	3.44	435	1092	161.7	794	175	28.1	169	23.2	134	24.1	60.2	6.98	35.9	4.94

Table A1. Cont.

Sample Name	Mg	Mn	Fe	Y	Th	U	La	Ce	Pr	Nd	Sm	Eu	Gd	Tb	Dy	Ho	Er	Tm	Yb	Lu
BR0417_B1_9	1927	666	1110	638	11.3	2.51	489	1243	179.2	859	194	30.5	177	25	142	26.2	65.7	7.55	39.8	5.41
BR0417_B1_10	1674	669	1066	793	14	3.1	607	1490	216	1027	239	32.6	214	30.2	174	32.5	82	9.46	49.9	6.72
BR0417_B1_11	2260	585	1073	569	16	2.83	398	984	149.1	735	165.2	30.5	156	21.7	122.6	22.9	59	7.12	37	4.98
BR0417_B1_12	1810	702	1084	1073	70	4.54	810	1990	288	1414	314	44.5	297	40.6	236	43.9	112	13.2	68.6	9.4
BR0417_B1_13	2329	601	1150	484	12.7	2.49	372	935	137	691	151	27.3	145	19.2	112.7	20.6	50.4	5.7	29.7	4.06
BR0417_B1_14	1959	639	1095	709	24.1	2.98	546	1328	194	944	209	33.2	194	27.1	155	29.2	74.3	8.6	44.5	6.08
BR0417_B1_15	1448	666	999	1125	58.5	4.26	859	2017	303	1512	354	45.2	326	44.1	249	46.5	119.3	14	72.4	9.81
BR0417_B1_16	1317	753	1067	958	18.6	2.84	765	1904	273	1313	285	33.9	270	36.7	208	38.3	96.7	11	57.2	7.8
BR0417_B1_17	1205	762	966	898	15.7	2.6	730	1832	274	1265	276	33.8	252	35.1	195	35	88.9	10.13	53.7	7.5
BR0417_B1_18	2240	562	1074	634	24.4	3.1	436	1030	164	803	192	32.1	171	24.6	133	25.1	65	7.8	40.6	5.7
BR0417_B1_19	1745	667	1052	782	13.2	3.29	609	1560	227	1036	237	35.1	217	30.4	170	32.4	80.5	9.4	48.2	6.53
BR0417_B1_20	1801	750	1035	703	14.7	3.28	511	1330	195	926	212	35.1	200	27.3	158	30.2	79	9.5	49.5	6.6
BR0417_B2_1	1871	658	1095	811	18.4	4.24	628	1572	225.6	1088	241.4	33	223	30.7	180.3	32.7	82.9	9.76	51.9	7.06
BR0417_B2_2	812	441	802	1204	20	4.23	989	2570	372	1762	381	27.7	340	47.2	270	49.3	126.8	14.4	73.9	9.65
BR0417_B2_3	777	447	707	1009	8.5	2.27	837	2200	320	1485	309	22.1	273	37.6	212	39.6	99.1	11.5	59	7.93
BR0417_B2_4	837	447	717	1047	11.9	3	783	2180	322	1443	314	24.3	289	39.2	224	40.1	102.1	12	58.6	7.75
BR0417_B2_5	1342	690	1028	1101	16.5	2.99	831	1709	270	1397	328	35.1	300	41.8	236	43.4	111.3	12.9	66.7	8.69
BR0417_B2_6	1714	588	1028	1079	37.3	3.62	742	1529	248	1345	325	42.8	315	41.8	235	42.8	107.9	13.1	66.9	9.1
BR0417_B2_7	2135	661	1221	639	13.9	3.17	464	1143	172.7	803	180.1	28.6	179	24	138.2	25.8	66.4	7.78	41.7	5.91
BR0417_B2_8	2129	643	1145	470	8.22	2.09	316	800	117.2	573	128.6	24.4	125.5	17.1	98.9	17.8	45.7	5.4	28.8	4.17
BR0417_B2_9	2151	653	1206	794	20.4	4.35	568	1448	209.5	1023	222	34.4	216	29.4	170	31.6	81.8	9.41	50.4	7.23
BR0417_B2_10	797	849	1018	1990	31.7	6.12	1397	3230	500	2590	607	60.5	560	78.8	446	81.3	198	22.6	118	15.7
BR0417_B2_11	1801	604	1116	939	20.6	3.67	651	1411	227	1193	274	39.8	257	36.7	210	39	99	11.5	59.5	8.11
BR0417_B2_12	1824	655	1156	901	19.5	4.18	660	1547	236	1123	253	38.1	248	34.9	198	37.4	95.7	11.4	59.8	8.22
BR0417_B2_13	1985	669	1225	736	17.9	4.21	548	1383	208	959	220	33.8	209	29.6	171	33.2	86	10.1	54.8	7.4
BR0417_B2_14	896	502	915	1537	42.1	5.94	883	2390	355	1870	448	43.3	440	62	358	66	167	19.2	100	13.4
BR0417_B2_15	1288	768	1111	817	12.6	3.01	604	1488	218	987	220	34	217	29.2	165	30.8	80.8	9.63	52.2	7.25
BR0417_B2_16	1420	677	1084	949	15.5	2.89	645	1368	222	1188	281	41.4	262	38	217	40.9	104	12	61.8	8.4
BR0417_B2_17	1931	633	1174	908	26.9	3.89	652	1530	226	1161	270	40.3	249	35.6	199	37.1	95	11	58	8.1
BR0417_B2_18	1820	581	1107	688	13.6	2.6	518	1277	189	902	203	28.1	189	26.2	151	27.5	71.6	8.2	42.6	5.92
BR0417_B2_19	1941	771	1221	672	13.4	2.81	463	1151	174	836	199	36.7	199	26.4	149	28	71.7	8.32	44.3	6
BR0417B3_1	1027	764	813	1229	19.2	3.92	827	2098	301.6	1528	343	39.2	326	44.5	262	48.5	123.3	14.27	75.3	10.19
BR0417B3_2	1549	690	1126	1202	55.3	5.2	860	2039	297.7	1530	346	44.5	340	44.1	250	46	117.6	13.74	73	9.93
BR0417B3_3	723	1056	867	1495	39.7	7.75	1350	3540	481	2180	448	44.9	425	56.9	327	60.4	162	19.6	103.9	13.8
BR0417B3_4	1254	783	1017	994	24.2	3.5	743	1893	279	1353	293	37	287	39.1	226	42.4	108.2	12.6	66.1	8.69
BR0417B3_5	1969	633	1137	748	16.7	3.75	535	1397	195.7	946	208	31.9	205	26.8	153.1	28.8	74.8	8.77	45.5	6.41
BR0417B3_6	2240	663	1096	915	24.4	4.61	659	1680	238.8	1167	267	40.2	250	33	193.3	35.5	88.7	10.37	56.8	7.82

Table A1. Cont.

Sample Name	Mg	Mn	Fe	Y	Th	U	La	Ce	Pr	Nd	Sm	Eu	Gd	Tb	Dy	Ho	Er	Tm	Yb	Lu
BR0417B3_7	675	982	821	1084	42.5	3.97	1022	2590	357	1637	336	32.5	313	41	234	43.9	116.7	14.1	73.1	10
BR0417B3_8	1432	761	1097	885	29.3	2.52	671	1710	249	1200	263	32.6	257	34.3	195	36.1	94	11.2	60.3	8.02
BR0417B3_9	1363	660	941	945	25.3	2.88	648	1549	231.6	1203	275	34.1	265	35.6	200.8	36.6	93.1	10.66	56.5	7.39
BR0417B3_10	1154	713	861	1451	28.8	4.85	978	2353	350	1770	409	46.6	398	53.4	309	57.5	146	17.1	88.5	11.91
BR0417B3_11	1723	699	1095	680	19.7	2.64	478	1262	180.6	867	192	31.7	190	24.8	139.2	26.3	66.9	7.81	43.5	5.87
BR0417B3_12	1738	767	1174	885	19.2	4.28	605	1559	230	1045	246	38.8	241	31.8	184	34.6	88	10.44	57.7	7.9
BR0417B3_13	1349	750	1022	993	19.9	4.37	766	1994	274	1308	275	32.8	275	36.4	208	39.2	101.6	11.87	63.4	8.31
BR0417B3_14	1085	791	1041	968	10.6	2.98	747	1950	262	1236	276	30.9	264	36.3	203	38.1	99.2	11.5	58.9	7.45
BR0417B3_15	2047	606	1107	690	50.5	3.59	487	1302	189.3	906	213	35	200	26.2	148.2	27.7	70.1	8.32	44	5.95
BR0417_A1_1	1186	630	840	1324	35.7	3.48	926	1843	299	1631	378	42.9	359	48.9	280	51.5	131	15.1	78.9	10.58
BR0417_A1_2	1479	598	768	911	33.8	3.28	639	1249	206.8	1109	256	36.4	243	33.8	193	36	92.5	10.97	58.3	8.07
BR0417_A1_3	1575	590	1034	1086	33.5	2.25	728	1295	225.2	1279	301	32.9	292	39	219	40.4	101	11.83	60	8.12
BR0417_A1_4	1207	649	908	1441	31.3	3.68	1049	2015	333	1777	405	40.3	394	53.9	300	54.6	139	16.1	85	11.5
BR0417_A1_5	1332	663	965	1001	24.2	2.4	729	1584	249.7	1274	293	34.6	275	38	212	38.4	98.7	11.45	59.2	8.06
BR0417_A1_6	753	458	743	1173	19.6	3.58	1055	2430	357	1676	337	25.4	311	42.2	239	43.4	115.1	13.7	71.7	9.6
BR0417_A1_7	1325	746	983	1030	18.1	2.84	803	1940	289	1398	295	32.7	281	38.5	217	39.8	103.6	11.9	62.8	8.66
BR0417_A1_8	1128	587	822	1437	48.4	4.16	1005	1959	330	1797	415	42.9	398	55.2	305	56.3	143	16.8	87.9	11.6
BR0417_A1_9	1318	733	973	973	25.9	2.59	706	1701	253	1241	278	32.5	271	36.5	208	38	99	11.6	61.5	8
BR0417_A1_10	1378	733	999	863	13.9	2.5	675	1653	243	1172	260	30.7	242	32.8	185	34.4	88.2	10.1	53.4	7.33
BR0417_A1_11	1335	745	1013	949	17.9	2.59	741	1790	262	1271	280	31.3	271	37.3	201	37.8	95.6	11.19	58.7	7.78
BR0417_A1_12	1314	791	994	1508	34.1	5.07	1392	3290	475	2168	455	47.1	420	56.5	314	58.6	150	17.6	93.1	12.5
BR0417_A1_13	1188	656	896	1174	16.8	2.43	862	1701	275	1457	322	35	314	43.8	242	43.3	110.6	12.6	66	9.01
BR0417_A1_14	1125	622	866	1714	53.8	4.02	1128	2033	350	1944	455	48.7	437	60.4	335	61.4	155.4	18.1	93.8	12.86
BR0417_A1_15	1267	639	954	1197	28.3	2.61	856	1667	274.6	1458	331	35	324	43.7	246	45.4	114.9	13.45	70.4	9.44
BR0417_A1_16	1676	737	950	753	18.4	1.72	437	780	142.8	870	214.1	32.8	209	28.5	158.6	28.8	73.3	8.46	42.2	5.79
BR0417_A1_17	990	830	1233	2097	30.6	7.29	988	2481	409	2123	541	26.7	538	81	464	85.9	209	23.5	117	14.8
BR0417_A1_18	1379	764	1012	1178	23.7	4.2	878	2030	304	1484	345	39.7	323	44.2	244	46.6	120	14.1	72.7	9.85
BR0417_A2_1	1185	633.1	900	1143	22.1	2.34	877	1681	283.1	1500	329.7	34.69	308.8	42.2	236.9	43.5	108.8	12.33	64.1	8.68
BR0417_A2_2	841	720	808	1305	25.3	2.87	1179	2950	441	2034	430	36.1	396	52.5	294	54.4	135.1	15	75.9	9.85
BR0417_A2_3	921	704	831	1047	37.2	3.06	847	2136	325	1530	340	37.4	310	42	236	43.5	110.5	12.63	64.4	8.46
BR0417_A2_4	929	773	883	2043	28.4	3.61	1586	3316	548	2834	635	47.4	592	80.7	456	84.9	212.9	24	121.1	16.08
BR0417_A2_5	939	751	888	1407	20.1	3.28	1260	3140	470	2166	471	41	417	57.1	315	58.2	144.8	16.2	81.1	10.64
BR0417_A2_6	1261	653	927	1084	43.6	3.39	886	2220	338	1593	353	40.6	323	43.7	249	46.3	117.7	13.6	70.9	9.51
BR0417_A2_7	1287	702	993	1194	29	3.65	1060	2670	403	1890	399	37.9	391	51.5	291	55.1	136	15.5	78.1	10.3
BR0417_A2_8	1345	712	1008	1535	66	5.8	1250	3180	486	2260	498	53.4	479	64	360	69.7	178	20.9	109	14.7
BR0417_A2_9	771	844	877	2103	69.7	9.47	1978	3604	592	3059	629	65.8	563	78.1	445	84.5	220.3	26.3	139	18.9
BR0417_A2_10	1031	636	874	1416	36	3.85	985	1938	337	1846	427	47.4	413	56.8	327	61.2	153.4	17.42	90.5	12.09

Table A1. Cont.

Sample Name	Mg	Mn	Fe	Y	Th	U	La	Ce	Pr	Nd	Sm	Eu	Gd	Tb	Dy	Ho	Er	Tm	Yb	Lu
BR0417_A2_11	988	810	963	1707	48.7	4.78	1439	3710	550	2650	575	47.1	522	70.7	405	74.4	183	20.2	106	13.9
BR0417_A2_12	928	745	864	1542	25.7	4.29	1353	3550	511	2400	508	44.2	471	62	354	65.7	166	19	98.1	12.9
BR0417_A3_1	898	820	1014	1311	46.9	5.75	1163	2490	383	1914	398	38	371	48.6	276	51	135	16.4	87	11.6
BR0417_A3_2	948	765	960	2141	81	4.86	1524	3380	530	2740	638	47.9	619	82.3	468	86.7	221	25.5	134	17.5
BR0417_A3_3	933	694	907	1752	56.7	2.96	1237	2395	394	2169	500	37.5	483	64.3	359	65.7	166	19.3	99	13
BR0417_A3_4	990	793	981	1689	60.3	3.79	1227	2990	441	2250	511	41.5	494	65.3	362	65.6	165	19	98	13.1
BR0417_A3_5	918	715	931	2031	42.8	3.98	1388	2817	461	2530	589	46.3	576	77.1	427	77.9	193	21.6	109.5	14.4
BR0417_A3_6	882	707	900	1606	26.5	2.98	1128	2389	374	1980	468	37.1	448	59.2	329	59.3	147.6	16.4	82.1	10.81
BR0417_A3_7	922	745	964	1601	31.4	2.57	1159	2630	408	2083	484	38	466	61.3	343	62.4	157	17.8	90	11.7
BR0417_A3_8	942	744	965	2001	71.7	3.95	1377	3090	481	2445	568	43.1	540	73.8	410	73.8	185	21.3	110.3	14.5
BR0417_A3_9	911	711	917	1577	28.6	2.89	1114	2435	383	1980	465	36.6	445	59.2	325	59.7	152	17.4	88.7	11.5
BR0417_A3_10	990	809	1022	1831	58.6	3.77	1313	3160	463	2350	541	41.2	508	69.2	387	71.4	180	21	108	14.3
BR0417_A3_11	881	697	908	2116	78	3.55	1376	2714	450.4	2529	596	47.1	586	77.5	427	76.5	188.3	21.25	106	13.87
BR0417_A3_12	937	730	999	1463	79	3.74	1053	2610	392	1939	447	37.9	423	55.9	306	55.4	137	15.3	77.6	10.25
BR0417_A3_13	934	719	920	1349	68.6	4.5	947	2380	346	1750	403	34.9	399	52.2	285	50.9	128	14.5	71.8	9.6
BR0417_A3_14	944	765	977	1327	37.1	2.38	991	2421	357	1751	403	32.4	383	50.3	277	50.9	126.9	14	71.3	9.3
BR0417_A4_1	1067	813	901	801	18.5	1.011	739	2174	276.7	1223	258.6	24.28	258.9	32.3	174.8	31.9	77.4	8.56	44.3	5.63
BR0417_A4_2	938	709	822	1037	37.3	1.845	895	2139	308.9	1492	331.5	28.46	318.4	40.42	223.7	40.6	99.5	11.04	57.2	7.35
BR0417_A4_3	970	738	901	1226	26.6	2.179	1042	2470	359.7	1724	380	32.4	368	47.3	259	46.7	115.1	12.93	66.8	8.74
BR0417_A4_4	995	724	821	915	27.9	1.772	728	1979	270.5	1281	281	25.8	285	36.3	200.3	36.4	88.7	9.69	49.4	6.47
BR0417_A4_5	954	728	814	1431	52.1	2.633	1216	2796	417.7	2033	446.2	39.9	442.8	57	315.6	57	139.9	15.68	79.8	10.28
BR0417_A4_6	931.8	700.5	802	1361	28.9	2.51	1174	2520	388	1912	421	35.7	416	52.8	291.5	53.2	131.7	14.64	75.7	9.79
BR0417_A4_7	1083	830	917	1157	19.33	1.968	1004	2844	372	1672	358	30.41	354	45	248.1	44.9	110	12.29	63.5	8.22
BRKBC_1	1469	509	1212	899	24.1	2.88	455	1099	168.3	870	210	28.6	223	29.5	166.5	31.5	83.6	9.51	48.1	6.65
BRKBC_2	886	501	1142	1046	27.5	2.94	1291	2850	408	1929	361	31.5	335	40.9	220	42	106.2	11.75	58.4	7.84
BRKBC_3	681	483	1036	1036	41.1	2.6	1186	2450	367	1829	349	31.2	333	41.3	220	41	100	11.19	54.8	7.34
BRKBC_4	1678	467	1183	829	37.1	2.55	419	958	157.4	865	215.7	33.9	235.7	30.6	170.1	32.4	80	8.67	44.7	6.15
BRKBC_5	1779	512	1441	1072	18.47	1.924	781	1740	259	1294	269	22.8	280	37	206	38.5	97.8	10.86	54.2	7.3
BRKBC_6	316	1009	647	2890	41.1	7.09	663	1840	341	1950	601	29.2	670	96.2	544	105.2	276	31.8	157	19.4
BRKBC_7	623	436.3	742	1186	15.5	3.45	1115	2278	340	1653	326	22.64	306	38.8	213.9	41.3	108.3	12.5	63.7	8.67
BRKBC_8	327.7	918	921	1557	21.6	3.55	1038	2460	368	1794	388	18.63	394	52.5	294	56.6	149.9	17.5	89	11.87
BRKBC_9	330	795	746	2810	42.6	10.03	1030	2620	467	2540	660	42.3	674	92.5	519	99	263	31.3	159.3	21.6
BRKBC_10	176	990	592	2489	32.2	4.91	799	2165	374	2034	563	30.6	595	83.4	474	90.6	228.9	26.3	132.7	16.86
BRKBC_11	162.1	1004	622	1830	11.99	2.56	471	1260	223.2	1241	371	18.95	410	58.7	335	63.4	164.7	18.94	93.4	11.82
BRKBC_12	561	581	1083	1862	32	5.08	1059	2470	390	2040	481	34.2	511	65.9	364	69.3	176.4	19.61	95	12.38
BRKBC_13	1462	496	1194	865	35.5	2.66	443	1008	164	880	214	34.1	239	31.8	175.6	32.3	81.3	9.24	46.7	6.48

Appendix B

LA-ICP-MS results of known and unknown Ordovician K-bentonites used for the ML test set.

Table A2. Results from the LA-ICP-MS analyses used as the test set. All elemental abundances are given in ppm.

Sample Name	Mg	Mn	Fe	Y	Th	U	La	Ce	Pr	Nd	Sm	Eu	Gd	Tb	Dy	Ho	Er	Tm	Yb	Lu
FP0417_D_1	788	454.8	909	654	11.13	3.9	605	1845	245	1036	208.8	17.07	193.2	24.96	136.8	25.27	63.6	7.17	36.56	4.76
FP0417_D_2	978	412.8	921	894	9.73	2.004	737	2101	293	1314	277.2	22.54	256.2	33.48	188.1	34.41	86.1	9.69	49.8	6.37
FP0417_D_3	1339	420	1245	712	11.84	3.14	650	2033	278.2	1180	242	26.5	212.3	27.68	153.1	27.69	69.7	7.84	40.4	5.15
FP0417_D_4	733	487	909	853	10.53	2.49	829	2542	328.7	1369	270.5	21.41	249.3	32.23	179.9	32.87	83	9.5	49.6	6.45
FP0417_D_5	1290	478	1232	754	10.04	2.75	723	2025	277.9	1210	247.4	21.35	224.2	29.2	161.1	29.5	74.1	8.48	44.3	5.7
FP0417_D_6	851	433	1082	847	7.89	2.166	703	2159	292.4	1245	260.1	20.96	246.6	31.67	179	32.69	81	9.1	46.7	5.98
FP0417_D_7	1120	381.5	1214	819	11.04	2.45	613	1793	253.7	1153	252.8	24.87	236.9	31.24	175.8	31.58	78.1	8.77	44	5.62
FP0417_D_8	724	472.4	1021	486	4.3	1.194	586	1621	208.3	842	156.4	12.32	137.1	17.42	97.1	17.86	46	5.27	28.07	3.714
FP0417_D_9	1251	464.2	1099	537	6.35	1.68	678	1850	239.5	976	180	14.24	157.5	19.7	108.9	20.05	51.6	5.98	32	4.21
FP0417_D_10	1161	393.1	1146	669	8.5	2.37	546.8	1645	229.1	1004	213.5	23.5	200.2	25.72	142.2	25.87	64.6	7.21	36.53	4.766
FP0417_D_11	1358	433.3	1312	645	9.25	2.6	502.7	1473	209.4	931	200.4	25.33	184.8	24.59	137.6	25.12	62.3	7.18	37	4.9
FP0417_D_12	1240	491.7	1156	569.8	10.1	2.224	790	2252	274.9	1072	189.2	15.13	162	20.23	112.4	20.88	55.1	6.57	35.55	4.77
FP0417_D_13	1065	456.9	1065	449.1	7.81	2.279	603	1727	216.9	857	152.7	21.36	136	16.93	92.2	17	44.2	5.24	28.7	3.93
FP0417_D_14	1259	364.4	1126	938	7.09	1.852	794	2228	322.8	1452	315.7	19.63	287.8	37.2	205.8	36.7	87.7	9.44	47.4	5.93
FP0417_D_15	1193	392.3	1303	662	6.82	1.611	527.9	1550	216.3	959	206.7	20.75	191.7	25.12	139.6	25.27	62.1	6.94	35.84	4.64
FP0417_D_16	1247	469	1383	862	6.33	4.37	539	1727	238	1041	237.7	13.91	234.8	32.7	189.2	34.9	87.7	10.03	51.4	6.53
BGX_1	1143	902	1565	1320	44.1	6.04	1435	4170	592	2640	537	21.59	454	53	296	54.5	136.6	15.04	78	10.14
BGX_2	1207	693	1318	1158	53.3	4.71	1256	3527	531	2417	478	16.23	408	48.7	261.7	46.4	116.8	12.75	64.8	8.32
BGX_3	1216	992	1525	1473	70.3	3.96	1087	3370	514	2394	510	23.9	466	59.7	328	59.1	148.3	16.71	89.2	11.61
BGX_4	1276	1065	1930	1530	54.7	6.3	1324	4280	637	2840	583	19.9	534	62.5	349	62.7	158	17.8	88.3	11.37
BGX_5	1462	1387	2100	2102	48.2	6.65	1038	3330	499	2272	542	16.48	517	71.5	420	80	212	25.1	131.9	17.11
BGX_6	1178	1123	1857	1540	44.9	3.85	1114	3560	540	2369	533	18.83	476	59.1	325	57.9	144.9	16.3	84.4	10.91
BGX_7	1618	1365	2119	2674	39.3	8.57	939	2854	478	2283	603	17.02	604	91.2	560	109.5	291	34.1	177.3	23
BGX_8	1465	1189	1990	1884	36.1	8.26	896	2939	455	2103	530	15.64	500	68.5	400	73.8	193.8	22.51	118.3	15.26
BGX_9	1759	1146	2026	1814	65.8	5.93	970	3067	488	2284	552	18.3	511	68.9	398	73.1	184.9	21.6	112.4	14.2
BGX_10	1452	1547	2219	2623	60.2	6.13	816	2800	458	2151	596	19.14	605	88.6	528	97.7	254	29.1	156.5	19.3
BGX_11	1279	1181	1646	1916	29.4	3.98	909	2860	449	2075	509	17.66	476	68.2	402	73.9	190	22.3	116.3	14.77
BGX_12	1365	1976	2281	3159	65.6	12.84	828	2940	471	2253	674	19.4	685	107.3	663	125.9	320	36.2	181	21.6
BGX_13	1469	1352	1931	2666	60.7	6.38	697	2122	360	1867	558	18.39	576	90	552	107.5	281	33.9	178.7	23
RMKB_16_1	737	452	976	774	7.47	1.92	726	2221	291.1	1232	249.9	19.32	229.6	29.57	165.7	30.4	75.6	8.61	43.8	5.73

Table A2. Cont.

Sample Name	Mg	Mn	Fe	Y	Th	U	La	Ce	Pr	Nd	Sm	Eu	Gd	Tb	Dy	Ho	Er	Tm	Yb	Lu
RMKB_16_2	638	500.1	880	498.4	8.53	1.601	728	2059	254.5	978	168.4	12.57	147.3	18.25	100.5	18.85	49.2	5.76	31.1	4.14
RMKB_16_3	835	436	933	593	3.8	1.17	528	1613	215.4	915	187.1	15.24	170.7	22.46	125.1	22.94	57.1	6.37	33	4.22
RMKB_16_4	864	431.1	1149	810	7.45	2.041	680	2126	284.6	1214	252.7	20.6	235.7	30.3	170.2	31.06	77.2	8.72	44.7	5.79
RMKB_16_5	823	461.3	1053	981	12.23	3.04	860	2604	353.2	1480	309	24.51	283.1	37.2	208.5	38.3	95.8	10.82	55.8	7.26
RMKB_16_6	718	456.3	972	690	6.84	11.3	650	1929	253	1087	224	17.63	207.8	27.09	151.6	27.98	69.2	7.65	38.9	5.02
RMKB_16_7	1030	471	1011	903	10.95	2.75	783	2500	327.4	1355	282	23.58	262	33.8	192.6	35.1	88.3	10.09	51.6	6.57
RMKB_16_8	940	431.7	962	774	10.18	2.7	644	1966	263.1	1124	236.9	21.44	214	28.01	158	28.99	73.4	8.42	43.6	5.62
RMKB_16_9	852	435	948	721	7.11	2.12	636	2026	269.2	1131	233.3	19.03	208.5	27.52	154.7	28.1	70.3	7.92	40.2	5.27
RMKB_16_10	828	452.6	941	1021	15.44	2.85	852	2535	341.7	1509	316.7	25.47	291.8	38.45	217.4	40	99.9	11.32	57.9	7.43
RMKB_16_11	866	457.3	927	565	7.16	1.904	431.4	1358	185.6	800	170.7	22.06	156.5	20.66	115.4	21.13	52.4	6.11	32.15	4.16
RMKB_16_12	850	426.9	900	888	10.37	2.26	723	2193	295.8	1298	268.4	21.65	251.5	33.6	185.9	33.9	84	9.47	48.8	6.25
RMKB_16_13	816	433.5	938	759	6.27	1.399	640	1929	258.7	1103	234.4	19	215	28.02	159.1	29.05	73.2	8.22	42.2	5.37
RMKB_16_14	778	464	925	635	7.64	2.23	628	1976	254.1	1001	198.8	18.02	181.1	23.22	132.4	24.23	61.2	7.05	36.7	4.75
RMKB_16_15	830	413	894	540	3.48	0.873	477	1479	191.8	816	166.7	14.32	151.7	19.55	112.4	20.27	49.9	5.61	28.8	3.65
RMKB_16_16	865	448	1124	805	9.29	2.39	721	2216	297.7	1255	257.7	19.95	231.6	30.44	168.9	31.1	77.4	8.85	45.9	5.85
RMMNE_1	188.8	795	625	1305	11.27	2.62	431.8	1253	214.5	1136	318.3	19.75	333	46.96	273.9	50.3	126.1	14.36	72.9	9.26
RMMNE_2	194.8	810	649	1132	6.42	1.736	401.6	1205	199	1017	279.7	18.66	286.6	40.1	235.6	43.09	108	12.38	62.1	7.91
RMMNE_3	385.5	508.5	854	1241	11.55	2.435	842.3	2140	345.8	1747	403.3	23.47	386.8	51.37	286.1	51.11	123.3	13.3	65.1	8.16
RMMNE_4	196.2	805.1	748	1224	8.58	1.985	380.9	1143	196	1023	297.8	18.4	312.1	44.5	258.7	47.67	118	13.27	66.4	8.46
RMMNE_5	208.9	871	729	1324	10.16	2.887	434.1	1427	234.5	1175	331.3	19.98	338.3	47.78	280.8	51.94	129.6	14.72	74.2	9.49
RMMNE_6	200	836	668	1528	12.7	3.51	537.4	1703	278.8	1401	376.9	23.55	383.6	54.9	320.6	58.8	147.5	16.9	85.9	10.91
RMMNE_7	191.8	810	642	1398	10.3	2.447	486.4	1458	247.5	1284	350.4	21.13	355.4	50.2	293.4	54.6	136.1	15.68	79.1	10.05
RMMNE_8	267.7	897	813	1387	13.09	3.471	578	1653	265.2	1337	355.8	22.78	362.1	50.95	296.7	54.8	136.7	15.56	79	10.09
RMMNE_9	204.3	863	720	1509	11.44	3.681	484.2	1641	264.6	1317	374.6	22.78	387.5	55.39	323.3	59.38	147.7	16.78	84.7	10.76
RMMNE_10	192.1	807.8	659	1966	19.66	4.87	577	1729	302.7	1596	469	28.22	488	70.3	415	77	191.1	21.98	110.8	14.01
RMMNE_11	197.3	834	685	1524	15.1	3.492	541.9	1647	273.4	1394	376.9	23.88	384.3	54.4	317.2	58	145.1	16.71	85	10.78
RMMNE_12	203.6	845	767	1390	9.85	3.079	453.8	1514	243.1	1235	345	20.9	352	50.53	294.9	54.37	135.7	15.4	77.8	9.89
RMMNE_13	197.3	841	679	1275	10.29	2.758	409	1359	218.1	1105	312.6	20	320.1	46.18	270.2	49.47	122.5	13.97	70.4	8.94
RMMNE_14	203.8	857	702	1261	8.95	2.602	424.4	1420	226.2	1131	317.2	19.59	318.9	45.59	266.3	49.16	123.7	14.21	71.3	8.99
RMMNE_15	1225	446.7	1277	1010	13.77	2.8	639.4	1587	255.5	1272	294.6	31.33	282.3	38.05	214.1	38.91	96.4	10.98	55.9	7.32
RMMNE_16	222	805.4	693	1635	32.7	3.83	485.5	1470	251.4	1337	391.4	23.81	410.5	59	346.5	63.9	158.4	17.97	89.9	11.39
RMMNE_17	194.4	819	900	1334	10.01	2.663	410.8	1325	219.9	1138	323.1	20.35	340.8	48.06	282.9	52.2	129	14.65	73.4	9.32
RMMNE_18	192.8	816.8	693	1872	23.1	4.5	567	1729	296.2	1545	451	26.67	466	66.9	393	72.4	180.9	20.61	104.3	13.28
RMMNE_19	188.3	797	625	1742	17.85	4.36	555.6	1610	281	1491	423.7	25.72	432.1	62.3	366.1	68	170.3	19.57	99.7	12.65
SPMBD_1	837	456	1006	1005	14.3	3.3	866	2710	360	1531	322	26.6	298	38.2	215.4	39.6	99.3	11.37	58.2	7.47
SPMBD_2	884	447	1027	740	6.74	1.81	636	1947	259.1	1105	236.2	19.03	211.6	28	156.5	28.7	72.2	8.17	41.5	5.38

Table A2. Cont.

Sample Name	Mg	Mn	Fe	Y	Th	U	La	Ce	Pr	Nd	Sm	Eu	Gd	Tb	Dy	Ho	Er	Tm	Yb	Lu
SPMBD_3	764	412.8	921	866	10.89	2.24	788	2139	297.5	1312	268.2	20.54	245.3	32	180.6	33.2	83.4	9.6	49.3	6.41
SPMBD_4	912	442.9	1097	1060	14.83	3.58	901	2798	377	1628	340	27.2	309	40.6	227	41.9	104	11.78	60.5	7.79
SPMBD_5	851	419.3	920	866	10.76	2.929	709	2130	287.1	1260	268	22.17	245.4	32.31	182.2	33.44	83.9	9.51	48.3	6.16
SPMBD_6	802	469.5	1075	790	8.57	2.18	691	2132	289	1223	252.7	20.62	232.4	30.03	169.9	30.9	76	8.59	43.8	5.62
SPMBD_7	824	437.4	939	875	33.4	9.04	798	2437	311.3	1284	255.6	20.73	225.1	29.66	170.5	32.56	87.4	11.54	69.7	9.81
SPMBD_8	798	416.5	876	780	7.51	1.88	716	2153	285.2	1198	246.8	19.47	222.1	28.61	159.4	29.23	73	8.35	43.1	5.51
SPMBD_9	746.4	413.1	880	779	10.26	2.331	697	1977	269	1177	239.3	19.63	221.1	28.08	160.7	29.27	73.2	8.4	43.8	5.66
SPMBD_10	811	412.4	891	1139	15.9	3.21	909	2689	372.8	1631	348.4	28.12	326.4	42.87	242.2	44.5	111.6	12.62	65	8.28
SPMBD_11	857	427.7	950	737	7.42	1.864	695	2110	272.8	1136	230	18.68	208.1	26.91	150.4	27.69	70	7.99	41.9	5.42
SPMBD_12	809	406.3	905	731	7.12	1.626	613	1786	243.6	1051	223.2	18.61	207.6	26.97	150.7	27.77	69.2	7.86	40.6	5.23
SPMBD_13	1178	480	1143	660	9.51	2.2	524	1582	217.1	989	212.5	26.52	197.7	25.39	141	25.89	63.7	7.15	38.4	4.97
SPMBD_14	756	392.1	855	801	9.37	1.952	694	1771	251.4	1161	246	20.4	225.1	29.22	166	30.26	75.8	8.73	44.93	5.77
SPMBM_1	237	781	607	3214	48.3	6.7	1241	2497	483	3047	812	40.5	832	117.4	670	122.1	303	34.2	171.4	22
SPMBM_2	156.6	906	547	3117	35.2	5.91	681	1541	313.6	2029	650	28.73	722	109.2	641	119.3	297	33.7	167.9	21.3
SPMBM_3	225	905	593	3600	52.5	7.32	702	1646	340.5	2207	730	32	817	124.2	737	137.6	343	39.3	198	24.9
SPMBM_4	190.8	841	603	2690	32.6	5.25	718	1955	359	2110	600	35.7	640	94.8	563	105.9	267	30.7	157.4	19.6
SPMBM_5	187.8	808	557	2320	33.1	4.84	624	1620	299	1769	524	30.1	553	83.4	485	90	225	25.8	129.5	16.38
SPMBM_6	163.3	927	567	1887	24.9	4.77	577	1619	282	1552	428	23.7	454	65.9	388	74.4	189	22.5	119	15.1
SPMBM_7	187.9	817	602	3110	38.2	9.75	752	2088	389	2310	704	40.2	763	113.5	672	125.9	318	36.8	188	23.2
SPMBM_8	184.8	810	582	2312	37.1	5.77	600	1582	293	1732	520	30.2	571	85	506	96.9	244	28.4	146	17.8
SPMBM_9	201.4	818	588	2018	14.8	4.08	604	1667	297	1686	471	27.8	484	71.8	418	77	201	23	117.7	15.3
SPMBM_10	190.4	838	587	2260	36.4	4.85	597	1657	296	1746	515	30.7	550	81.6	490	93.3	236	27.6	141	17.7
SPMBM_11	183.3	819	574	1999	29.9	3.83	531	1466	270	1585	469	28.6	507	76.4	455	85.7	214	24.3	123	15
SPMBM_12	175	950	588	1513	12.3	3.79	464	1388	237	1296	362	21.1	375	55.1	328	63.6	166	19.7	102	12.7
SPMBM_13	179.7	1002	575	3260	42.6	8.17	786	2230	410	2330	707	35.8	757	114.6	687	128.9	325	38	198	24.5
SPMBM_14	197.3	772	612	3240	51.8	10.5	812	2045	392	2400	728	42.2	777	116.2	697	133.1	338	39.8	208	25.9
SPMBM_15	204	792	593	3260	50.7	8.88	785	1960	384	2350	719	39.4	779	116.7	690	130.4	326	37.7	195	24.5
RM2JTH_1	220.5	789	543	3720	87.4	8.34	912	2069	441	2770	858	46	897	137.6	828	157.7	401	47.2	238	30.8
RM2JTH_2	199.6	800	562	2847	98.5	5.84	755	1769	356.8	2239	686	39.3	692	105.8	626	116.1	290	33.3	168	21.8
RM2JTH_3	228.3	816	621	4815	98.2	13.78	1146	2679	558	3536	1116	59	1174	178.5	1069	198.9	498	57.9	290	37.2
RM2JTH_4	195	896	680	2570	48.7	6.58	746	2280	407	2230	651	38.1	666	100.1	601	113	287	33.7	170	21
RM2JTH_5	1021	354.1	988	1579	47.6	4.81	1157	2255	385	2111	480	27.4	459	62.9	355	64.6	158.5	17.7	87.3	11.11
RM2JTH_6	292	753	686	2983	205	11.26	1337	3205	595	3310	814	53.6	765	110.4	641	121.1	315	38.1	201	26.8
RM2JTH_7	195	946	624	3030	48.6	10.6	998	3090	526	2820	758	46.8	758	115.8	682	130	324	38.1	193	24.7
RM2JTH_8	181.6	818	572	3860	87.6	12.7	952	2436	479	2950	924	50.6	963	148	892	170	431	50.8	254	31.6
RM2JTH_9	190.3	897	616	1900	24.8	6.23	638	2055	352	1808	498	31	508	75.2	450	83.8	210	24.8	123	16.2

Table A2. Cont.

Sample Name	Mg	Mn	Fe	Y	Th	U	La	Ce	Pr	Nd	Sm	Eu	Gd	Tb	Dy	Ho	Er	Tm	Yb	Lu
RM2JTH_10	160.9	940	531	2530	43.1	7.42	833	2180	415	2370	659	35.2	636	95.2	568	107.3	277	33.5	175	22.8
RM2JTH_11	186	840	586	2127	60.2	6.12	594	1698	301	1728	525	31	533	82.6	487	93.1	234	27.7	139	18.1
RM2JTH_12	193.1	876	598	1598	34	3.57	513	1589	270	1442	401	24.7	402	60.5	353	66.1	165	19.2	96.6	12.7
RM2JTH_13	186.4	832	584	2314	43.5	5.16	602	1662	317	1833	559	34.1	580	88.6	531	99.1	250	29.3	148	18.9
RM2JTH_14	366	649	807	1815	108	4.55	893	2370	403	2110	541	30	522	75	433	79.7	198	22.6	112	14.4
RM2JTH_15	384	597	778	3250	138	7.88	1589	3270	618	3710	952	50.8	905	130.6	749	138	339	37.8	183	23.1
RM2JTH_16	224.1	815	580	2017	54.2	4.81	515	1383	264	1565	482	29.2	511	76.7	460	86.3	216	25.4	126	16.2
RM2JTH_17	183.6	757	537	1158	57.5	1.2	312.3	728	144.8	906	277	17.02	293	43.9	259	48.4	120	13.76	67.1	8.64
DNMNE_1	212.2	826	752	1352	11.45	3.107	483.1	1516	244.4	1259	336.3	20.79	341.2	47.89	280.2	51.85	128.7	14.8	75.7	9.6
DNMNE_2	180.5	977	659	1277	14.68	2.827	507.7	1601	249.5	1244	318.2	18.59	316.9	44.61	260.4	48.1	120.3	13.98	72	9.23
DNMNE_3	1426	675	3770	1156	19.6	2.763	738	2147	320.7	1516	342.6	28.19	332.3	43.76	249.5	45.43	111.6	12.56	64.2	8.27
DNMNE_4	196.5	812	697	1556	16.6	3.34	484.2	1511	252.4	1345	378.7	23.01	391	56	326.5	60.4	149.2	17.09	86.4	11.05
DNMNE_5	206.6	831	847	1300	11.44	2.58	415.1	1350	222.9	1136	319.7	19.7	332.2	46.8	273.6	50.8	124.7	14.3	72.6	9.3
DNMNE_6	217.4	780	703	1427	32.7	3.16	617.3	1712	279.8	1462	373.9	23.66	371	51.4	295.4	54.5	135.4	15.58	80	10.16
DNMNE_7	194.7	787	651	1403	12.78	3	528.6	1504	247.9	1330	353.6	23.64	357.8	49.86	291.2	53.7	133.6	15.42	78.9	10.09
DNMNE_8	169.9	935	665	1562	18.6	2.683	421.6	1319	222.7	1200	352.8	18.28	378.5	54.6	322.2	59.6	148	16.91	86.2	10.85
DNMNE_9	163.2	960	655	1735	18.1	2.615	392.8	1215	213.2	1181	379.7	14.68	428.1	61.93	369.9	68.9	167.7	18.9	94.1	11.84
DNMNE_10	213	790.6	666	1597	25.8	3.167	528.7	1540	263.4	1410	396.2	23.42	411.2	57.64	338.4	62.5	154.5	17.74	90.2	11.57
DNMNE_11	269.5	748	820	1278	11.23	2.508	464.4	1351	222.6	1183	322.1	20.06	329.1	46.18	268.5	49.61	122.1	13.93	70.4	8.95
DNMNE_12	514.3	464.2	1006	1261	13.89	3.054	948	2724	401.1	1924	424	26.27	398.6	51.56	285.9	51.18	122.7	13.44	66.4	8.35
DNMNE_13	166.3	944	698	1612	33.1	2.87	563.7	1618	267.9	1435	388.7	21.6	393.9	55.6	327.6	60.4	150.8	17.52	89.6	11.3
DNMNE_14	193.4	774	668	2157	42.5	5.46	594.6	1647	301.3	1711	514.5	30.46	549.2	78	463.6	85.7	212.7	24.11	121.4	15.4
DNMNE_15	199.6	893.6	603	1978	23.9	3.67	507.8	1447	259.8	1477	449.9	22.41	478.5	69.5	415.3	77.1	190.9	22.07	111.6	14.1
DNMNE_16	409	762.8	737	1546	42.3	3.05	467.2	1306	232.2	1291	377	22.78	395.1	55.51	326.4	60.9	150.5	17.15	86.9	11.07
DNMNE_17	268	824	876	1152	15.32	2.355	460.1	1444	228.4	1152	301.8	18.88	299.3	41.75	242.7	44.48	110.5	12.58	64	8.14
DNMNE_18	759	596	1307	1229	15.9	3.68	854	2599	374.1	1756	385.9	26.24	367.6	47.5	270.6	48.6	118.9	13.08	66	8.37
DNMNE_19	199.1	824	664	1030	5.95	2.01	357.1	1174	191.9	959	262.2	16.29	265.7	37.33	220	40.5	100.5	11.41	58.1	7.34
DD_NE_1	819	411	670	1340	21.7	3.19	1022	2623	386.6	1830	391.1	31.53	374.4	49.1	275.8	50.6	127.8	14.66	74.9	9.49
DD_NE_2	774	404.8	706	2513	78	10.75	2064	4580	715	3430	721	53.6	659	88.8	504	92.9	238	27.95	147	18.69
DD_NE_3	778	424.1	721	984	12.21	2.183	887	2459	329.4	1494	300.5	24.04	281.7	36.8	204.8	37.9	95.7	10.93	56.9	7.24
DD_NE_4	926	453.5	787	655	5.31	2.24	569	1759	231.5	993	203.1	17.03	187.6	24.49	134.6	24.6	62	6.89	35.69	4.49
DD_NE_5	683	470.9	634	850	23.45	3.71	975	2734	343.6	1454	268.1	21.06	241.4	30.54	169.3	31.73	82.6	9.72	52.2	6.92
DD_NE_6	808	397.3	642	1063	13.62	2.47	824	2039	301.3	1460	312.9	25.25	294.7	39.3	217.5	40.3	101.1	11.56	59.2	7.49
DD_NE_7	874	396.6	760	792	7.91	1.518	618	1469	224.3	1097	232.1	21.11	221.7	29.21	164.7	29.97	75.4	8.43	44	5.6
DD_NE_8	870	430.7	663	819	8.55	1.866	658	1953	264.5	1166	244.8	20.75	234.8	30.44	169.3	30.88	76.9	8.64	44.4	5.67
DD_NE_9	883	415.5	686	738	7.36	1.676	611	1767	242.2	1100	230.6	17.08	217.8	28.01	153.1	28.3	69.9	7.73	39.5	4.97

Table A2. Cont.

Sample Name	Mg	Mn	Fe	Y	Th	U	La	Ce	Pr	Nd	Sm	Eu	Gd	Tb	Dy	Ho	Er	Tm	Yb	Lu
DD_NE_10	843	451.9	726	942	12.6	2.16	771	2236	301.5	1358	284.5	23.37	269.7	35.35	196.9	36.3	91.1	10.43	53.7	6.84
DD_NE_11	754	397.4	637	799	7.61	1.405	667	1647	240.8	1143	239.4	18.87	225.1	29.35	165.2	30.39	76	8.49	43.5	5.56
DD_NE_12	796.2	392.5	625	875	10.22	1.841	694	1757	255.1	1198	255	20.48	236.5	31.45	175.9	32.18	80.9	9.16	47.4	6.08
DD_NE_13	791.3	382.3	624	887	8.24	1.495	711	1773	261.2	1246	266.9	21.27	250	32.82	184.1	33.72	84.9	9.51	48.7	6.26
DD_NE_14	807	440.2	696	1758	42.6	6.7	1450	3856	545	2530	533	42.8	497	65.6	369	67.9	172.1	20.04	104.7	13.36
DD_NE_15	897	430.9	710	1017	13.09	2.36	799	2324	317.6	1424	299.7	24.82	284.5	37.3	209.5	38.4	95.6	10.99	56.6	7.13
DD_NE_16	722.4	474.5	965	666	8.01	1.72	763	2049	266.6	1111	207.9	16.18	185.6	23.38	130.9	24.17	62.1	7.31	38.9	5.15
DD_NE_17	713.2	399.5	602	1151	17.72	2.761	1014	2421	357.9	1684	343.8	26.48	319.3	41.86	235.5	43.43	109.6	12.37	64.3	8.26
DD_NE_18	800.8	396.2	643	886	13.54	3.31	733	1842	267.1	1241	259.9	21.65	244.1	32.08	181	33.1	84.8	9.74	50.7	6.43
DD_NE_19	790.9	385.1	672	1053	11.3	1.891	830	2000	299.3	1450	309.9	24.78	294.8	38.61	216.9	39.69	99.4	11.23	57.4	7.37
DD_NE_20	724.8	409.5	629	2136	58.1	8.31	1637	4010	602	2905	622	49.6	595	78.9	448	82.7	207.6	24.27	126.3	16
DV_E_1	1190	606	1201	1072	20.6	3.98	751	1780	270	1357	307	42.8	304	41.3	233	44.5	116	13.6	70.2	9.6
DV_E_2	1152	574	1176	1196	21.3	3.96	823	1860	302	1504	346	47.8	333	46.2	261	49.3	125	14.5	73.9	9.7
DV_E_3	1291	583	1264	1519	33.4	7.7	1030	2560	404	1910	444	66.7	436	59.2	332	64	164	19.7	104	14.5
DV_E_4	1016	573	1128	2161	70.4	8.2	1900	4380	633	3090	659	66.3	632	85.3	491	95	248	29.7	157	20.9
DV_E_5	1192	590	1179	925	13.6	3.68	636	1548	240	1189	257	35.8	249	33.5	193	36.2	95	11.4	58.7	8.2
DV_E_6	1246	621	1203	985	22.5	4.7	693	1710	274	1308	290	42.4	285	38.9	221	42.9	108	13	69	9.5
DV_E_7	1161	602	1158	961	15.2	3.26	644	1620	246	1217	264	35.2	264	35.2	204	39	103	12.3	64.2	9.1
DV_E_8	1085	526	1085	1073	121	5.2	724	1750	272	1341	300	40.6	296	39.9	230	44.2	114	13.5	74	10.2
DV_E_9	1398	473	1202	996	19.1	3.14	725	1810	279	1334	301	36.3	292	39.5	224	41.8	106	12.2	62.5	8.4
DV_E_10	1188	550	1148	1025	24.9	3.99	689	1596	250	1239	286	41.4	275	36.6	213	40.4	103	12.5	67	9.5
DV_E_11	1040	522	1080	984	23.9	3.31	670	1603	246	1221	279	35.9	265	37.2	205	38.3	96.4	11.35	57.5	7.78
DV_E_12	536	625	971	1905	31.2	5.85	1557	3790	572	2710	587	43.1	562	76.2	426	79.7	196	21.7	107.7	13.8
DV_E_13	1288	612	1198	978	21.4	3.88	668	1670	251	1204	279	41.5	281	37.4	215	41.6	108	12.5	65.5	8.9
DV_E_14	1045	526	1053	1034	18.1	2.05	675	1652	255	1260	305	31	308	42.5	239	44.8	112	12.1	61.5	8.1
DV_E_15	1287	607	1237	1169	47.1	5.8	792	2004	310	1521	332	48.9	332	43.6	249	48.5	124	14.4	77	10.9
DV_E_16	1121	554	1150	1240	30.5	4.36	830	1920	299	1546	354	44.2	347	47.7	268	50.6	128	14.9	78	10.4
DV_E_17	1046	487	1017	1201	23.7	3.57	789	1644	273	1441	323	39	326	43.5	249	46.1	117	13.7	71.6	9.43
DV_E_18	1134	557	1160	909	21.6	5.55	879	2170	308	1398	276	27.3	256	33.8	188	35.4	89.7	10.41	53.2	7.48
TH0616M_1	410	931	887	791	10.63	2.85	510	1826	252.6	1116	241.5	17.92	213.6	28.71	164.1	30.4	77.6	9.11	48.3	6.25
TH0616M_2	530	746	1370	898	11.95	3.64	646	2530	323	1349	299	21.7	257	34.2	189.9	35	86	9.66	50	6.19
TH0616M_3	249.1	997	805	849	10.05	11.39	550	2115	275.1	1140	246.9	18.56	228	30.02	172.2	31.3	80.3	9.31	48.6	6.12
TH0616M_4	916	686	1361	689	8.38	12.79	165.5	713	110.7	540	143.8	23.15	140.4	19.9	123.6	25	69.4	10.04	64	9.37
TH0616M_5	372	1034	1033	839	5.77	2.015	514	2015	268.7	1170	257.6	13.02	246.3	32.1	180.2	33.2	81.3	9.1	47.6	6.11
TH0616M_6	248.8	994	742	660	5.51	2.06	389	1393	186.1	813	184.9	19.33	171.8	23.12	131.3	24.15	60.8	7.1	37.4	4.87

Table A2. Cont.

Sample Name	Mg	Mn	Fe	Y	Th	U	La	Ce	Pr	Nd	Sm	Eu	Gd	Tb	Dy	Ho	Er	Tm	Yb	Lu
TH0616M_7	232	1152	704	1050	8.13	2.37	411	1700	232	1052	266	17.2	251	35.7	207	39.1	97	11.34	57.6	7.38
TH0616M_8	249.2	849	743	1201	25.3	6.96	834	2960	400	1707	360	25.7	321	43.2	243	45	113.1	13.29	69.8	9.13
TH0616M_9	275	1011	805	869	10.03	3.46	439	1553	221.5	999	240	19.88	219	30.2	174.8	32.1	80.6	9.57	50.4	6.43
TH0616M_10	228.1	1021	737	1304	16.15	4.89	576	2320	320	1410	351	23.2	312	44.3	256	48	124	14.61	76	9.75
TH0616M_11	196.5	1169	716	1119	7.87	2.99	439	1801	249	1128	292	18.1	272	38.5	221	41.5	103.7	12.04	63	8.05
TH0616M_12	243.5	1053	816	1117	8.54	2.91	509	2081	281	1244	303	20.02	284	39.2	226.5	42.3	104.8	12.28	63.1	8.03
TH0616M_13	1047	551	1300	706	6.02	1.88	645	2209	271.2	1130	232.2	19.35	207	26.7	149.1	27.3	68.4	7.78	40.3	5.22
TH0616M_14	230.7	998	806	1055	7.35	2.73	437	1656	240.6	1059	270	15.72	252.7	35.6	208.2	38.7	97.5	11.41	59.3	7.56
TH0616M_15	881	796	1263	896	10.98	14.65	675	2430	321	1371	293	21.3	266	35.6	198	35.5	85.8	9.68	49.6	6.29
TH0616M_16	371	997	967	660	7.1	2.5	510	1868	243.8	1012	208.7	17.24	178.6	24.11	134.1	24.95	63.4	7.57	40.1	5.35
TH0616M_17	202.4	1128	699	913	7.92	2.58	573	2040	279.5	1219	270.3	18.35	248.6	33.06	185.5	34.8	86.6	10.08	51.8	6.66
TH_M_1	1060	812	1009	959	12.82	3.394	702	2021	312.3	1482	326.5	22.23	306.7	40.19	218.8	39.52	96.8	10.7	54.2	7
TH_M_2	417	964	757	1169	23.06	4.83	1031	2999	440	1908	382.5	28.51	347	43.2	237.8	44.3	117.7	14.43	78.5	10.89
TH_M_3	986	874	992	1759	14.56	4.32	717	2093	350.8	1716	439	28.77	458.2	66.1	391.3	74.4	187.6	21.35	107.8	13.73
TH_M_4	798	720	822	1377	11.62	2.64	839	2470	397	1862	434	29.62	413	55.3	307.3	55.3	134.1	14.74	74.2	9.22
TH_M_5	1075	842	1084	1330	11.12	5.23	692	2092	347.4	1635	390	19.99	381.2	52	298.4	54.5	136.1	15.41	79.2	10.29
TH_M_6	191.8	1023	501	1453	15.4	3.44	582	1744	294.8	1422	374	22.54	374	52.9	306	56.6	141	16.26	84.5	10.69
TH_M_7	1109	942	1192	1546	16.42	5.84	697	2278	373.2	1770	434	22.09	434	60.1	350.6	65.7	167.7	19.14	98.9	12.61
TH_M_8	549	1036	756	1538	45.3	12.18	1074	3244	489	2255	478	34.4	437	58.1	321	59.7	155.3	18.32	102.3	13.75
TH_M_9	217	933	533	1477	15.44	4.43	652	2044	337.1	1609	404	25.67	391	53.7	310.3	56.9	143.2	16.46	84.8	10.87
TH_M_10	262.2	842	593	1317	17	4.32	835	2486	392	1833	413	30.92	390	51.4	289	52.4	130.6	14.6	74.6	9.5
TH_M_11	214.3	898	522	944	7.89	2.475	547	1590	252.7	1158	269.9	20.99	255.6	34.52	196	35.66	89.2	10.19	52.1	6.8
TH_M_12	1311	457	811	709	8.68	2.623	559	1548	238.2	1057	235.4	24.54	221.6	28.67	156.8	28.01	68.8	7.53	38.6	4.97
TH_M_13	447.8	965	763	1024	10.07	3.24	867	2539	381.8	1680	348.7	23.58	318.5	41.06	222.9	40.2	100.3	11.2	57.1	7.45
TH_M_14	992	834	1028	1213	13.63	3.64	751	2212	352	1614	370	23.29	368	49.8	280	50.3	124.4	13.81	69.2	8.66
TH_M_15	896	445.9	677	887	11.4	3.64	723	2018	297	1304	282	21.8	265	34.1	188.2	34.4	86	9.61	49.3	6.44
TH_M_16	216.7	924	561	1897	19.2	5.05	584	1764	306	1620	472	28	470	69.4	395	73.4	181.2	20.7	105.7	13.63
TH_M_17	1003	832	1008	1190	11.75	3.75	694	2102	327.1	1538	369.3	23.74	357.5	48.8	275.1	50.2	124	13.6	68.7	8.79
TH_M_18	224.4	949	535	1069	7.62	2.023	597	1789	281.8	1303	321.9	21.4	305	41.63	235.3	42.8	106.4	11.97	60.5	7.62
TH_M_19	750	642	861	1058	13.64	3	980	2588	375.6	1667	346.3	28.8	323.4	41.8	231.3	41.9	103.9	11.56	59.7	7.64
THD_1	873	458.3	688	780	9.65	2.21	673	1878	281.8	1214	258.6	21.18	242.1	31.02	169.5	31.52	78.9	8.9	46.1	5.91
THD_2	850	459	736	1792	68.1	11.1	1586	4160	615	2800	595	46.4	541	70.9	389	72.8	187	22	119.1	15.04
THD_3	888	455	670	729	7.41	1.88	635	1776	259.7	1112	232.6	19.34	210.5	27.5	150.9	27.9	70.3	8.05	41.5	5.37
THD_4	869	481	683	954	15.92	3.18	806	2327	341	1489	305	25.3	293	38	207.7	38.5	96.7	10.98	56.8	7.35
THD_5	711	515	761	710	17.08	3.16	985	2704	354.4	1408	250.1	19.63	220.8	26.67	145.5	27.53	72.8	8.68	48.1	6.39
THD_6	920	468	717	1004	14.12	2.86	812	2393	360	1545	332	26	310	40.8	222.1	41	101.8	11.37	58.3	7.48

Table A2. Cont.

Sample Name	Mg	Mn	Fe	Y	Th	U	La	Ce	Pr	Nd	Sm	Eu	Gd	Tb	Dy	Ho	Er	Tm	Yb	Lu
THD_7	892	451.7	670	970	14.71	3.63	807	2350	338	1489	313.7	25.61	300.5	38.8	212.4	39.5	98.3	11.05	57.4	7.39
THD_8	852	461.3	653	964	12.49	4.57	824	2395	350	1534	319	24.65	297	38.1	209.7	38.8	97.9	10.96	56.5	7.35
THD_9	748	478	648	993	18.57	3.81	975	2787	400	1675	330.6	25.52	309.6	39.3	215.7	40.4	102.4	11.67	62.2	8.17
THD_10	800	469.2	678	937	10.83	1.978	830	2153	326.5	1462	308.4	24.65	287.7	37.16	203.7	38	95.1	10.81	56.8	7.39
THD_11	868	445.5	682	1001	18.29	3.23	932	2674	380.4	1628	330.9	26.37	302.9	38.97	215	40.2	100.7	11.61	60.7	7.85
THD_12	872	503	709	957	10.54	2.41	818	2356	345.7	1498	312	25.36	299.4	38	209.8	39.2	96.9	10.98	56.4	7.28
THD_13	839	465	673	842	17.28	4.08	814	2332	334.1	1408	284.5	23.02	263	33.6	182.2	33.9	85.3	9.65	50.5	6.45

Appendix C

LA-ICP-MS settings for the different runs.

Table A3. Big Ridge Kb-A (laser runs A1–A3), Big Ridge Kb-B (laser runs B1–B3), Big Ridge Kb-C, Rochester Millbrig and Deicke, Brickyard Millbrig, Dickeyville Elkport.

Instrument	Parameters	Setting
<i>Thermo Scientific iCap Qc ICP-MS</i>		
	RF Power (W)	1550
	Cool gas flow rate (mL/min)	1400
	Carrier gas (Ar) flow rate (mL/min)	723
	Carrier gas (He) flow rate (mL/min)	700
<i>Cetac G2 LSX-213 Laser Ablation System</i>		
	Laser type	Nd: YAG
	Wavelength (nm)	213
	Laser energy (%)	30
	Pulse repetition rate (Hz)	10
	Shutter delay (s)	10
	Burst count	800
	Ablation time (s)	90
	Washout time (s)	30
	Spot size (µm)	25

Table A4. Big Ridge Kb-A A4, Big Ridge Millbrig M1–M4, Big Ridge Deicke D1–D7, Brickyard Deicke, Decorah Deicke, Fort Payne Deicke and Millbrig, Tidwell Hollow Millbrig, Dickeyville Millbrig.

Instrument	Parameters	Setting
<i>Thermo Scientific iCap Qc ICP-MS</i>		
	RF Power (W)	1550
	Cool gas flow rate (mL/min)	1400
	Carrier gas (Ar) flow rate (mL/min)	723
	Carrier gas (He) flow rate (mL/min)	650
<i>Cetac G2 LSX-213 Laser Ablation System</i>		
	Laser type	Nd: YAG
	Wavelength (nm)	213
	Laser energy (%)	30
	Pulse repetition rate (Hz)	10
	Shutter delay (s)	10
	Burst count	600
	Ablation time (s)	60
	Washout time (s)	30
	Spot size (µm)	50

Table A5. Fort Payne Millbrig Bottom, Bruton Gap Kb-X, Tidwell Hollow Deicke.

Instrument	Parameters	Setting
<i>Thermo Scientific iCap Qc ICP-MS</i>		
	RF Power (W)	1550
	Cool gas flow rate (mL/min)	1400
	Carrier gas (Ar) flow rate (mL/min)	723
	Carrier gas (He) flow rate (mL/min)	800
<i>Cetac G2 LSX-213 Laser Ablation System</i>		
	Laser type	Nd: YAG
	Wavelength (nm)	213
	Laser energy (%)	30
	Pulse repetition rate (Hz)	10
	Shutter delay (s)	10
	Burst count	700
	Ablation time (s)	60
	Washout time (s)	30
	Spot size (µm)	50

References

1. Mao, M.; Rukhlov, A.S.; Rowins, S.M.; Spence, J.; Coogan, L.A. Apatite Trace Element Compositions: A Robust New Tool for Mineral Exploration. *Econ. Geol.* **2016**, *111*, 1187–1222. [[CrossRef](#)]
2. O’Sullivan, G.; Chew, D.; Kenny, G.; Henrichs, I.; Mulligan, D. The trace element composition of apatite and its application to detrital provenance studies. *Earth Sci. Rev.* **2020**, *201*, 103044. [[CrossRef](#)]
3. Takashima, R.; Kusakawa, H.; Kuwabara, S.; Orihashi, Y.; Nishi, H.; Niwano, M.; Yoshida, T. Identification of the source caldera for a Pliocene ash-flow tuff in Northeast Japan based on apatite trace-element compositions and zircon U-Pb ages. *J. Volcanol. Geotherm. Res.* **2020**, *401*, 106948. [[CrossRef](#)]
4. Sell, K.B.; Samson, S.D. A tephrochronologic method based on apatite trace-element chemistry. *Quat. Res.* **2017**, *76*, 157–166. [[CrossRef](#)]
5. Sell, B.K.; Samson, S.D.; Mitchell, C.E.; McLaughlin, P.I.; Koenig, A.E.; Leslie, S.A. Stratigraphic correlations using trace elements in apatite from Late Ordovician (Sandbian-Katian) K-bentonites of eastern North America. *Geol. Soc. Am. Bull.* **2015**, *127*, 1259–1274. [[CrossRef](#)]
6. Takashima, R.; Kuwabara, S.; Sato, T.; Takemura, K.; Nishi, H. Utility of trace elements in apatite for discrimination and correlation of Quaternary ignimbrites and co-ignimbrite ashes, Japan. *Quat. Geochronol.* **2017**, *41*, 151–162. [[CrossRef](#)]
7. Kolata, D.R.; Huff, W.D.; Bergström, S.M. *Ordovician K-Bentonites of Eastern North America*; Geological Society of America: Boulder, CO, USA, 1996; Volume 313.
8. Huff, W.D. Ordovician K-bentonites: Issues in interpreting and correlating ancient tephros. *Quat. Int.* **2008**, *178*, 276–287. [[CrossRef](#)]
9. Huff, W.D.; Kolata, D.R. Correlation of the Ordovician Deicke and Millbrig K-Bentonites Between the Mississippi Valley and the Southern Appalachians (1). *AAPG Bull.* **1990**, *74*, 1736–1747. [[CrossRef](#)]
10. Bergström, S.M.; Huff, W.D.; Kolata, D.R.; Bauert, H. Nomenclature, stratigraphy, chemical fingerprinting, and areal distribution of some Middle Ordovician K-bentonites in Baltoscandia. *Gff* **1995**, *117*, 1–13. [[CrossRef](#)]
11. Dronov, A.; Huff, W.; Kanygin, A.; Gonta, T. K-bentonites in the Upper Ordovician of the Siberian Platform. *Ordovician World. Cuad. Del Mus. Geomin.* **2011**, *14*, 135–141.
12. Fanning, C.M.; Pankhurst, R.J.; Rapela, C.W.; Baldo, E.G.; Casquet, C.; Galindo, C. K-bentonites in the Argentine Precordillera contemporaneous with rhyolite volcanism in the Famatinian Arc. *J. Geol. Soc.* **2004**, *161*, 747–756. [[CrossRef](#)]
13. Lowe, D.J. Tephrochronology and its application: A review. *Quat. Geochronol.* **2011**, *6*, 107–153. [[CrossRef](#)]
14. Carey, A.; Samson, S.D.; Sell, B. Utility and Limitations of Apatite Phenocryst Chemistry for Continent-Scale Correlation of Ordovician K-Bentonites. *J. Geol.* **2009**, *117*, 1–14. [[CrossRef](#)]
15. Emerson, N.R.; Simo, J.A.; Byers, C.W.; Fournelle, J. Correlation of (Ordovician, Mohawkian) K-bentonites in the upper Mississippi valley using apatite chemistry: Implications for stratigraphic interpretation of the mixed carbonate-siliciclastic Decorah Formation. *Palaeogeogr. Palaeoclimatol. Palaeoecol.* **2004**, *210*, 215–233. [[CrossRef](#)]
16. Kolata, D.R.; Huff, W.D.; Bergström, S.M. Nature and regional significance of unconformities associated with the Middle Ordovician Hagan K-bentonite complex in the North American midcontinent. *Geol. Soc. Am. Bull.* **1998**, *110*, 723–739. [[CrossRef](#)]
17. Bolton, M.S.M.; Jensen, B.J.L.; Wallace, K.; Praet, N.; Fortin, D.; Kaufman, D.; De Batist, M. Machine learning classifiers for attributing tephra to source volcanoes: An evaluation of methods for Alaska tephros. *J. Quat. Sci.* **2019**, *35*, 81–92. [[CrossRef](#)]
18. Carniel, R.; Guzmán, S.R. Machine Learning in Volcanology: A Review. In *Updates in Volcanology-Transdisciplinary Nature of Volcano Science*. Nemeth, K., Ed.; IntechOpen: London, UK, 2020. [[CrossRef](#)]
19. Rosenau, N.A.; Herrmann, A.D.; Leslie, S.A. Conodont apatite $\delta^{18}\text{O}$ values from a platform margin setting, Oklahoma, USA: Implications for initiation of Late Ordovician icehouse conditions. *Palaeogeogr. Palaeoclimatol. Palaeoecol.* **2012**, *315*, 172–180. [[CrossRef](#)]
20. Quinton, P.C.; Herrmann, A.D.; Leslie, S.A.; MacLeod, K.G. Carbon cycling across the southern margin of Laurentia during the Late Ordovician. *Palaeogeogr. Palaeoclimatol. Palaeoecol.* **2016**, *458*, 63–76. [[CrossRef](#)]
21. Quinton, P.C.; Law, S.; Macleod, K.G.; Herrmann, A.D.; Haynes, J.T.; Leslie, S.A. Testing the early Late Ordovician cool-water hypothesis with oxygen isotopes from conodont apatite. *Geol. Mag.* **2017**, *155*, 1727–1741. [[CrossRef](#)]
22. Keller, M.; Lehnert, O. Ordovician paleokarst and quartz sand: Evidence of volcanically triggered extreme climates? *Palaeogeogr. Palaeoclimatol. Palaeoecol.* **2010**, *296*, 297–309. [[CrossRef](#)]
23. Hall, M.; Frank, E.; Holmes, G.; Pfahringer, B.; Reutemann, P.; Witten, I.H. The WEKA data mining software: An update. *ACM SIGKDD Explor. Newsl.* **2009**, *11*, 10–18. [[CrossRef](#)]
24. Witten, I.H.; Frank, E. Data mining: Practical machine learning tools and techniques with Java implementations. *ACM Sigmod Rec.* **2002**, *31*, 76–77. [[CrossRef](#)]
25. Valls, R.A. *Exploring Geological Data with Weka, CoDaPack, and iNZight: Graphical Instructions*; CreateSpace Independent Publishing Platform: Scotts Valley, CA, USA, 2017.
26. Quinlan, J.R. *C4. 5: Programs for Machine Learning*; Elsevier: Amsterdam, The Netherlands, 2014.
27. Herrmann, A.D.; Haynes, J.T.; Robinet, R.M.; Konzett, J.; Emerson, N.R. Insights into the tectonostratigraphic setting of the Southern Appalachians during the Blountian tectophase from an integrated geochemical analysis of magmatic phenocrysts in the Ordovician Deicke K-bentonite. *Lithos* **2021**, *398–399*, 106301. [[CrossRef](#)]

28. Rice, W.F. *The Systematics and Biostratigraphy of the Brachiopoda of the Decorah Shale at St. Paul, Minnesota*; University of Minnesota: Minneapolis, MN, USA, 1985.
29. Herrmann, A.; Haynes, J.T. Ordovician of the Southern Appalachians, USA, Pre-symposium Field Trip. *Stratigraphy* **2015**, *12*, 203–251.
30. Haynes, J.T. *The Ordovician Deicke and Millbrig K-Bentonite Beds of the Cincinnati Arch and the Southern Valley and Ridge Province*; Geological Society of America: Boulder, CO, USA, 1994; Volume 290.
31. Paton, C.; Hellstrom, J.; Paul, B.; Woodhead, J.; Hergt, J. Iolite: Freeware for the visualisation and processing of mass spectrometric data. *J. Anal. At. Spectrom.* **2011**, *26*, 2508–2518. [[CrossRef](#)]
32. Schmitt, R.A.; Smith, R.H.; Lasch, J.E.; Mosen, A.W.; Olehy, D.A.; Vasilevskis, J. Abundances of the fourteen rare-earth elements, scandium, and yttrium in meteoritic and terrestrial matter. *Geochim. Cosmochim. Acta* **1963**, *27*, 577–622. [[CrossRef](#)]
33. Stormer, J.C.; Pierson, M.L.; Tacker, R.C. Variation of F and Cl X-ray intensity due to anisotropic diffusion in apatite during electron microprobe analysis. *Am. Mineral.* **1993**, *78*, 641–648.
34. Fletmetakis, S.; Berndt, J.; Klemme, S.; Genske, F.; Cadoux, A.; Louvel, M.; Rohrbach, A. An Improved Electron Microprobe Method for the Analysis of Halogens in Natural Silicate Glasses. *Microsc. Microanal.* **2020**, *26*, 857–866. [[CrossRef](#)] [[PubMed](#)]
35. Haynes, J.T.; Melson, W.G.; Kunk, M.J. Composition of biotite phenocrysts in Ordovician tephra casts doubt on the proposed trans-Atlantic correlation of the Millbrig K-bentonite (United States) and the Kinnekulle K-bentonite (Sweden). *Geology* **1995**, *23*, 847–850. [[CrossRef](#)]
36. Willman, H.B.; Kolata, D.R. The Platteville and Galena groups in northern Illinois. *Circular* **1978**, 75.